CY-05-243

Attachment 2
Haddam Neck Plant
Task 3 Groundwater Modeling Report, November 2005

December 2005

TABLE OF CONTENTS

LIST OF TABLES

LIST OF FIGURES

LIST OF APPENDICES

Connecticut Yankee Groundwater Modeling done in Support of Decommissioning

1 Introduction

Stratex, LLC, has developed a suite of groundwater models to support the decommissioning of the Connecticut Yankee Atomic Power Company's (CYAPCO) Haddam Neck Plant (HNP) nuclear power plant. This work was done under contract with CH2M-Hill and has relied heavily on their data and interpretations of the geology and hydrogeology of the site and surrounding area.

This modeling work complies in most respects with the following ASTM Standard Guides: D 5447 –04 (Application of a Ground-Water Flow Model to a Site-Specific Problem; D 5490 –93 (reapproved 2002) (Comparing Ground-Water Flow Model Simulations to Site-Specific Information); D 5609 –94 (reapproved 2002) (Defining Boundary Conditions in Ground-Water Flow Modeling); D 5610 –94 (reapproved 2002) (Defining Initial Conditions in Ground-Water Flow Modeling); D 5611 –94 (reapproved 2002) (Conducting a Sensitivity Analysis for a Ground-Water Flow Model Application); D 5718 –95 (reapproved 2000) (Documenting a Ground-Water Flow Application); D 5880 –95 (reapproved 2000) (Subsurface Flow and Transport Modeling). Any significant deviations from these standards are noted in the report.

The modeling work began in October 2004 and has included several episodes of model improvement over the initial steady-state flow model that was delivered at the end of 2004. In the winter of 2005, the steady-state model was improved. A transient model to evaluate the response to Connecticut River tidal fluctuation was developed and initially calibrated. A series of modeling scenarios were then completed to assist in decision-making relative to the method of dewatering and refilling the PAB and RHR excavations. In June, work began to refine the steady-state model and simulate the September 2004 pumping test at AT-1. In July 2005 solute transport runs were made to evaluate potential future impact from leaving radionuclide-contaminated rock in place under the Tank Farm. This work product presents the refined models that have been calibrated to May tidal fluctuations, the September 2004 pumping test, and an approximate "steady-state" operational condition. It reports on the calibration statistics for these models. The models are used to simulate several scenarios that include particle tracking.

1.1 Scope and Objectives

Development of a numerical simulation tool for HNP was identified as a requirement under the *Phase 2 Hydrogeologic Characterization Work Plan* (Malcom Pirnie, 2002). The modeling activity is described generically under specifications for Task 3 of the work plan. The primary use of the simulation tool is to identify potential groundwater flow paths that can be used to assess groundwater monitoring needs (e.g., monitoring well locations, well depths and screened interval depths.). Although the model has the capability to simulate fate and transport of specific constituents of concern, this capability

is deemed to be less useful than the flow simulation due to the "mature" state of the groundwater contamination conditions at HNP and the on-going removal of primary and secondary sources of contamination. A "mature" groundwater contamination condition is indicated by generally stable or diminishing contaminant concentrations in groundwater and apparent cessation of release of contaminants from identified source areas (or removal of those sources). The modeling activity for HNP has, therefore, focused most intensively on simulation of groundwater flow pathways, rather than reactive transport simulation of the migration of specific contaminants along those pathways.

The scope and objectives of the modeling activity are described in the following subsections.

1.1.1 Scope

The scope of this modeling exercise is broad, covering the HNP in three dimensions and multiple operational periods. Although the primary focus area is the industrial area occupied by the reactor and generating station, the overall model domain has to be sufficiently large to define reasonable boundary conditions. Because the Connecticut River acts as a discharge boundary and HNP is located near that boundary, the model domain was extended to encompass hydrologic drainage basins on both the north and south sides of the Connecticut River. The scope of the modeling activity is summarized in the following bullets:

- Physical Scope of the Model
    - The area of known contamination (i.e., extending from a short distance inland of the industrial area to the Connecticut River in the north-south direction, and from the Emergency Operations Facility to about 0.5 mile southeast of the industrial area in the east-west direction) is modeled in detail.
    - The major drainages on the north and south sides of the Connecticut River, with HNP in the approximate middle, are included for completeness.
    - In the vertical dimension, the model incorporates unsaturated and saturated hydrogeologic units from the ground surface to approximately 700 feet below ground surface. This includes a perched unit underlying the HNP parking lot area, an unconfined aquifer unit that includes the near-surface unconsolidated formation overlying bedrock as well as portions of the shallow bedrock in some locations, and a confined aquifer unit that resides primarily within the deeper bedrock formation.
    - Include the capability for simulation of reactive transport of specific substances of concern.
- Temporal Scope of the Model
    - Historical Operating Conditions (pre-closure)
    - Maximum Dewatering Conditions (during demolition activities)
    - Post Closure Conditions (after completion of demolition activities)

The physical scope of the modeling exercise is intended to be sufficiently robust to incorporate hydrologic boundary conditions in all three dimensions. The temporal scope is intended to provide indication of the effects of long-term and short-term hydrologic transient events over the course of plant operation and closure. The scope of the modeling activity is supported by the hydrogeologic conceptual site model.

1.1.2 Objectives

Several general and specific objectives were defined for the modeling activity. These objectives support data needs identified for groundwater monitoring and for strategic evaluation of the post-closure conditions at HNP and are listed below:

- General Objectives
  - Produce a numerical simulation tool that is representative of observed site conditions at HNP.
  - Produce a numerical simulation tool that can be used to illustrate groundwater flow regimes within the hydrogeologic formations identified at HNP.
  - Produce a simulation tool that can support assessment of fate and transport of specific substances of concern originating at specific source term locations.
  - Assess the potential impacts of changing conditions related to termination of plant operations and performance of decommissioning activities at HNP.
- Specific Objectives
  - Incorporate the results of on-site measurement of site-specific conditions (e.g., groundwater elevation, aquifer characteristics derived from hydrologic testing).
  - Simulate the effects of operation of site dewatering systems, including historical operation of the reactor contaminant foundation mat dewatering sump, and active dewatering systems associated with plant demolition and removal actions.
  - Simulate the flow of groundwater (and associated soluble substances) across the HNP, including both horizontal and vertical flow within adjacent and overlying hydrogeologic units.
  - Simulate the effects of site boundary conditions (e.g., the discharge boundary effect of the Connecticut River).
  - Simulate the effect on groundwater flow of HNP subsurface structures that intersect bedrock and create boundaries to flow within the unconsolidated formation underlying the plant.
  - Calibrate the simulation to observed site conditions.

1.2 Modeling Software

MODFLOW and MT3DMS are porous media models, but can be adapted to model flow and transport in fractured media. Appendix A includes a discussion of the application of the porous media model to the Connecticut Yankee site. Most of the model development has been done with a regional model covering a large area on both sides of the Connecticut River valley. However, some smaller submodels were created to study specific problems in the plant area. The flow models are constructed using the "original" 1996 version of MODFLOW as developed by the US Geological Survey (USGS). Groundwater Vistas (GWV), GW4, Version 4.18, has been used as the pre- and post-processor. Groundwater Vistas allows for easy creation of submodels through the telescopic mesh refinement routine (TMR). Particle tracking used the USGS MODPATH program with pre- and post-processing by Groundwater Vistas. Solute transport was implemented using MTD3MS developed by the US Army Corps of Engineers (COE) with pre- and post-processing by Groundwater Vistas.

ArcView was used to prepare data sets and present some of the final results. Rockware was used to develop the geologic database and create gridded surficial unit surfaces and cross sections to aid in the 3-dimensional design of the model. Surfer was used to grid and contour some of the data.

1.3 Base Map Preparation and Spatial Location of Data

The model base maps were constructed in ArcView, utilizing a large amount of data available through the internet and through personal contact with Connecticut state agencies. These data were provided in Connecticut State Plane projections, 1983 mean sea level datum in feet. Some data were available for the site in NAD 1927 datum. The site base map, which was not in native ArcView format, was fit to the orthophoto quadrangle maps, which were available in ArcView format. There are discrepancies in elevation between the USGS map and the detailed site topo map in the uplands north and east of the IA. Near the IA, we have used some of the more detailed site topo by digitizing it and importing it as blanked Surfer files. We also had to digitize the elevation of the bottom of the Connecticut River and other tidal inlets from the US Coast and Geodetic Survey navigation chart.

Other Arc "shape files" of USGS map topography, streams, surficial geology, bedrock geology, soils, and wetlands were all utilized for offsite data. More detailed bedrock geology data (London) and site-specific boring data were used to develop the onsite model parameters. Offsite well and groundwater level data sources included USGS and Connecticut State publications of well data in the area, plus a survey of local area wells by CY personnel. The USGS publications listed well locations according to lat-long and interpolated elevations from USGS topographic maps. The local area well survey data locations were digitized in UTM and ground elevations were visually interpolated from the topo map. It is not clear how closely the suggested well locations lie to the actual

locations since many wells are shown literally on the house they pertain to, which is unrealistic. USGS map locations in lat-long were transformed to UTM coordinates and all offsite well data were transformed from UTM to the site coordinate system of Connecticut State Plane Coordinates 1983 (feet). Figure 1 shows the location of geologic data points that were utilized.

1.4 Rockware Database and Surfer used for Geologic Data and Layer Elevations

All offsite and onsite geologic drilling data were entered in a Rockware geologic database system. Offsite bedrock elevations were estimated by starting with the ground surface topography reverse-interpolated from the USGS shapefile, and subtracting soil thickness, based on ArcView interpretation of surficial geology and soils maps. Estimated bottom elevations of the sand and gravel aquifer adjacent to the Connecticut River were digitized from USGS and State publications. These calculated elevations were then compared with "known" data points, and adjusted as necessary. The detailed site bedrock topography in the industrial area of the plant (IA) area was taken from a Surfer grid file developed in support of the Task 1 Summary Data Report (CH2M-Hill, 2004) and provided to me by CH2M-Hill, then transformed into the site coordinate system and blanked to only apply to the area of plentiful data. The bedrock surface in areas away from the IA, but still on the site, were estimated using other historical site borings and interpolated with Rockware software, then blanked in Surfer only to cover the area among and immediately surrounding the borings. The detailed IA map and the surrounding area map were then gridded together in Surfer to smooth out the transitions. Finally, the regional bedrock surface and the composite site bedrock surface map were gridded together in Surfer to smooth out the interface. The final map was imported into Groundwater Vistas through the final Surfer grid file and reverse-interpolated into the proper layer and cells. The bedrock surface topography is shown on Figure 2.

2 Model Discretization

A large regional model was constructed to encompass the Connecticut Yankee site. It is apparent from looking at the topographic map of the area that groundwater that flows through the plant site could begin at great distance (over two miles) to the northwest along the crest of a bedrock ridge. Rather than attempt to guess at the flux of groundwater flow entering the site from the north and using constant flux boundaries to represent that flux contribution, we elected to include a large naturally-bounded area that would, by its nature, determine the flux. This was particularly important in light of the transient modeling we have done where determining the flux under variable stress conditions would have been quite difficult.

Looking to the southwest side of the Connecticut River, a persistent concern has been whether, and under what conditions, any contamination that was generated at the site could be intercepted by wells on the opposite side of the River. Again, rather than trying to apply constant flux boundary conditions southwest of the area of interest on the southwestern side of the River, we have extended the model boundaries on that side out to natural boundaries that would allow the model to distribute the flux appropriately

along the River valley walls. In this way, we can apply any theoretical combination of pumping stresses on the south side of the River without having to worry how a nearby boundary condition specification would affect the results.

The regional model was discretized into the standard rectangular finite-difference grid, but with irregular spacing. The regional model contains 176 rows, 127 columns, and 9 layers. Cell widths varied from 6.25 feet to 510 feet. A Groundwater Vistas routine was used to provide the transitional spacing to minimize numerical errors resulting from the change in cell widths. Figure 3 shows the finite-difference grid overlain on the USGS base map. The TMR models all have the same layering, but different numbers of rows and columns depending on what was being simulated.

The top three layers of the model consist of soil. The layers are of equal thickness (total soil thickness divided by 3) in most areas except near the IA where sufficient data were available to define specific geologic units such as the "red fine sand" unit. This approach for discretizing the layering of the soil was taken after careful consideration of the high degree of variability in the stratigraphic sections from place to place. It appeared to be too difficult and speculative, given the sparse density of data away from the IA, to develop a reliable correlation of surficial units on a regional scale. The bedrock is divided into 6 layers with thinner layers at the top and increasing layer thickness with depth. Layers are numbered from the top (1) to the bottom (9). Total bedrock thickness is 600 feet as follows: Layer 4—25 feet thick; Layer 5—25 feet; Layer 6—37.5 feet; Layer 7—37.5 feet; Layer 8—75 feet; and Layer 9—400 feet.

Glacial till is treated as an aquitard under layer 3 of the model with an equivalent K'/B value ("leakance" or vertical hydraulic conductivity, K' or Kz, divided by an assumed one-foot thickness). The Kz value can be varied spatially to account for localized differences in vertical hydraulic conductivity divided by till thickness (K'/B) but lacking high quality data on this variability, it was treated as a constant throughout the model (0.2 feet per day per foot) except is 0 on the north side of the discharge tunnel and under most of the containment. .

3 Boundary Condition Specification

There are a variety of boundary conditions used in the modeling. No-flow boundaries (a special case of constant flux boundaries where flux is constant at zero--also called Neumann or Type 2 boundaries) are placed around the outside of the naturally-defined limits of the regional model, and under the bottom of the models. As calibration proceeded, certain areas of the uplands that were predicted by the model to become "dry" were then fixed as no-flow cells in order to improve the convergence of the regional model, which is highly non-linear as all layers including 7 and above were allowed to be simulated as "unconfined" if the layers above were not predicted to be saturated. There are a total of 115,990 active cells in the regional flow model.

The Connecticut River and tidal tributaries within the model area are treated as constant head cells (also called Dirichlet or Type 1 boundaries) with a defined elevation of 1.74

feet NGVD (the site datum) for average annual recharge-based simulations. The CH2M-Hill reported levels (data recorded every 15 seconds) were adjusted for the May 2004 tidal simulation and the September 2004 pumping test simulation (see Appendix B). There are a total of 3664 constant head cells in the regional flow model. They are defined only in layer 1 of the model.

Streams and upland rivers were defined as "drains" (also called Cauchy or Type 3 boundaries). This is a condition that allows discharge from the modeled groundwater system into the drain, but when the water table is predicted by the model to drop below the defined drain bottom elevation, there is no water contributed by the stream to the model. The resistance to discharge into the drain is controlled by the "conductance" value assigned to each drain cell. The drains were digitized in segments based on the USGS map elevations along streams defined on the State shape file of "streams". Because some of the cells in the periphery of the model are large (510 feet by 510 feet) and the slopes are steep in many areas, the linear interpolation routine caused some "drain" cells to be defined below the top layer of the model where soil thickness was very thin. Certain dewatering well locations and the containment foundation mat drain and sump were also treated as drains so that the flow into the cell would be determined by the hydraulics rather than setting a withdrawal rate that could have caused the cell to go dry. There are a total of 2423 drains in the model.

Several small water bodies within the model area are treated as general head boundaries (GHB), which allow for transfer of water both into and out of the cell, at a rate depending on the conductance of the cell interface and the difference between the predicted head in the cell and the specified head of the water body. The stormwater control pond on the site just east of the Emergency Operations Facility (EOF) was treated as a general head boundary because of the obvious flow into the pond on the north side and the flow out of the pond on the south side. The conductance on the north side of the stormwater pond is a high conductance of about 4000 feet squared per day, but a lower rate of only 25 square feet per day on the south side. A swamp located in the highlands north of the main parking lot was also treated as a GHB because it was perennially wet and supplied springs that discharged part of the way down the hill above the parking lot. Some areas of ponded water in the drains at the foot of the rock-cut north of the containment building and tank farm were also treated as small water sources (conductance of only one square foot per day) as they collected the seepage from the hillside and the ponded water slowly recharged the ground to the south.

Concrete foundations that extend through all or part of the soil on the site in the IA were treated as equivalent "barrier walls", which are analytical elements used to simulate impervious or nearly impervious barriers to horizontal flow. These wall elements were placed in the top three layers of the model in locations given on a map provided by CH2M-Hill. Because the containment mat foundation drain extended under the containment walls in places, the wall segments were not included entirely around the containment in layer 3. There is a difference between the position of walls in place during operation and the position of wells following operation and that is reflected in the appropriate way in each simulation.

The plant well (Well B on the peninsula) that supplied most of the water during decommissioning was included in the model during the runs made for calibration during decommissioning. The leachfield that discharged the septic sewage during the early part of the decommissioning was also included as a source of water in the appropriate location on the peninsula (applied as additional recharge water over the leachfield area).

Boundary conditions for the top layer of the model are shown for the entire model on Figure 4. Figure 4A shows the local distribution of no-flow cells and dry cells in the top layer of the model under average annual recharge, pre-demo conditions. Boundary conditions in the site area are shown on the various plots showing results of the special modeling scenarios (such as Figures 31-34).

4 Hydraulic Conductivity and Recharge Parameterization

The Site Conceptual Model[1] report forms the basic framework for parameterizing the model. That report describes the basic geology and hydrogeology of the site in terms of how recharge flows through the site to discharge to the river. The information contained within the Site Conceptual Model report was relied upon heavily in constructing this mathematical representation. See that report for details on the conceptual model.

Regional surficial and bedrock geology units for the offsite area were interpreted from ArcView shapefiles obtained from the State of Connecticut. The London[2] map was obtained from CH2M-Hill. The initial parameterization for hydraulic conductivity consisted of 26 separate units, although many were later combined to simplify model calibration. We combined units from London's detailed bedrock geology map into units that, by their description, should perform similarly from a hydrogeologic viewpoint. In the simplification process for initial calibration, we lumped units into: top bedrock layer (layer 4); second bedrock layer (layer 5); bottom bedrock layer (layer 9); and layers 6, 7, and 8 having similar properties except with respect to particular linears. One extensive north-south trending linear element in the bedrock portion of the model near column 71 is a low permeability zone representing the Cremation Hill Fault zone (treated isotropically at 0.005 feet per day). In the process of calibrating the site model we added several other specialized unit codes for hydraulic conductivity of localized rock areas.

Since there are fabric elements in the rock that favor both vertical and horizontal flow, we oriented the grid north-south to conform to the predominant direction of bedrock vertical foliation strike to permit the use of anisotropy (the final rock hydraulic conductivity anisotropy has north-south values equal to twice the east-west values). Appendix C contains some rose diagrams and stereonets of observed fracture and photolineament orientations on and near the site. Several north-south linears were simulated with higher-

[1] CH2M-Hill, 2005, Site Conceptual Model

[2] London, D., 1989, Bedrock Geology of the Moodus Seismic Area, South-Central Connecticut, with map, Report of Investigations No. 11, State Geological and Natural History Survey of Connecticut, Connecticut Department of Environmental Protection, Hartford, CT

than-average hydraulic conductivity. One N60E linear was incorporated (from containment to MW-102). The model X-axis is oriented east-west (true north); the model Y-axis is oriented north-south.

Several areas of higher-than-average bedrock hydraulic conductivity were included in layer 5 to conform to observations that a clustering of monitoring wells and piezometers responded to each other during pressure transients. The depth within the rock cross sections on which the linears were placed was varied to find optimum calibration fit. Of all the site parameters, the horizontal and vertical location of linears was the most important in calibrating to the observed bedrock monitoring well record. Although we believe that the rock below the 200-foot depth is generally relatively low permeability, matching vertical gradients suggests that 3 of the inferred site linears probably extend vertically into the deep rock layer. This is not inconsistent with the fact that many high yield bedrock wells in crystalline rock in New England have been found in the 500 to 700 foot depth range.

Initial hydraulic conductivity estimates for rock and soil were based on experience, past measured site values reported by CH2M-Hill, and various packer tests and the September 2004 pumping test. Values were varied within reasonable ranges to calibrate the model to observed water level readings in monitoring wells. Table 1 gives the final hydraulic conductivity values used in the model. The regional distribution of the soil layer hydraulic conductivity is given in Figures 5, 6, and 7 for Model layers 1, 2, and 3, respectively. Figures 8, 9, 10, 11, 12, and 13 show the hydraulic conductivities used in the rock for model layers 4, 5, 6, 7, 8, and 9, respectively.

Generalized soil units consist of: sand and gravel; red fine sand; sand and gravel; silty sand; sand fill; silt and clay; sandy till; thick till; and thin till. The spatial differentiation of precipitation recharge was developed from the USDA soil maps, available in an ArcView shape file. The soil map was manipulated in ArcView to combine soil types of similar recharge capability, then the aggregated map reverse-interpolated into the top layer of the model. Several USGS and State publications provided good guidance on net average annual recharge rates for various surficial geologic units and these were correlated and applied to the various soil series groupings, based on texture and parent soil material. Average annual recharge distribution for the steady-state operational history modeling is shown in Figure 14. Recharge in all models was applied to the top active layer of the model. Areas where rock was shallow had a low applied recharge rate. Areas of thicker soil are capable of storing recharge at higher average rates and slowly releasing it at a rate it can be absorbed by underlying bedrock. The IA area in the post-demolition state is simulated as having an average annual recharge rate of 0.0035 feet per day or 15.3 inches per year. Table 2 gives the detailed average annual recharge values for the pre-demolition state.

5 Transient and Solute Transport Parameters

Because transient simulations were performed, it was necessary to estimate and then calibrate storativity or storage coefficient and specific yield (Sy). Because of the high

relief in the area encompassed by the model, specific storage (Ss) was specified rather than the storage coefficient (specific storage is equal to storage coefficient per foot of aquifer thickness). Specific storage works more accurately with unconfined model layers. The May 2004 matching of tidal response and the September 2004 pumping test were used to calibrate Ss and Sy. Figure 15 shows the zonation of specific storage for the middle soil layer (Model layer 2). Table 3 shows the specific yield and porosity of the zones defined on Figure 15. Almost all of the soil is in Zone 1. Almost all of the rock is in Zone 2. Table 3 gives the detailed specific storage, specific yield, and porosity used in the transient and solute transport simulations.

Although not part of the scope of this modeling report, some solute transport simulation work has been performed in support on ongoing remedial actions at the site. We report the parameter values used in those evaluations done to date in this report solely to aid the client in providing a reference for this information. As part of the evaluation of the potential solute transport from the bedrock contamination found under the "tank farm", solute transport simulations required the specification of porosities, dispersivities, bulk densities, and of Kd (linear isotherm assumptions) values for the two isotopes studied in details (Sr-90 and Cs-137). The Kd and bulk density values used are derived in Table D-1 of Appendix D. Specific gravity and other data used to estimate bulk density were supplied by CH2M-Hill. The dispersivities were chosen to be rather modest to prevent excess spreading: longitudinal dispersivity (D_L) = 10 feet; transverse dispersivity (D_T) = 1 foot; and vertical dispersivity (D_V) = 0.1 foot throughout the entire model domain.

6 Model Calibration and Verification

The calibration of the models was based primarily on a comparison of "observed" and "predicted" heads on a long-term average annual basis. Some reported offsite well data were discarded because it was obvious that the reported water level was the depth at which the first water-producing fracture was encountered, rather than the static level. Offsite data that were not obviously erroneously reported as static water levels are still subject to a high degree of uncertainty due to potential errors in well location (which, on the very steep terrain, can produce errors of tens of feet in elevation) and uncertainty over how a single reported water level at the time of the reading relates to the long-term average annual water level. The typical error in well location is probably 100 feet on slopes averaging 20%, or 20 feet. The typical deviation in reported well water elevation in relationship to the long term average is probably 5 feet. The typical error in taking off elevation from the USGS topographic map is one-half the contour interval or 5 feet. On the other hand, the error in estimating the average annual elevation of site data that has been surveyed and for which at least a partial continuous water level record is available is probably less than 2 feet. Therefore, the offsite data ("Group 2" data on the graphs) were assigned a generous weight of 0.2. The site groundwater data ("Group 1" data on the graphs) taken from piezometers with at least 3 months of record were assigned a weight of 1.0. Calibration residuals (observed values minus predicted values) for the steady-state regional model are calculated by multiplying the difference between observed and predicted head by the weighting factor for each "target" or observation point. This puts more weight on the site-based data that are more reliable.

The model was calibrated for both steady-state and for transient conditions. We did not do a typical "verification" run to check a set of heads or fluxes under a different set of stresses than those used for calibration. The steady-state model was calibrated first. Then the May 2004 transient tidal response model was calibrated with changes made to hydraulic conductivities, placement of linears, specific storage, and specific yield. Finally, the September 2004 pumping test was used as a further basis for calibration and hydraulic conductivities, specific storage, and specific yield were modified slightly more in the area of influence of the pumping test. Following these final changes, the steady-state model and May 2004 transient simulation model were run again to produce the final calibration statistics presented here. So, in reality, the steady-state and May 2004 models would actually qualify as "verification" runs, although we are treating them as calibration runs.

All calibrations and sensitivity analyses were done with the regional model. TMR models were only used to simulate various scenarios of interest, or to do particle tracking. The transient simulations were based on matching individual monitoring well responses with the typical rise and fall (4-foot typical tidal range) of the Connecticut River and with a pumping test in the surficial deposits of the site. The client desired a model that was capable of estimating times to dewater or rewet real or hypothetical excavations on the site, so determining the approximate range of specific yield and specific storage coefficients could only be done through transient calibration. Also, it is well known that tidal response is a function of transmissivity and storativity and the response to tide change provided an excellent opportunity to refine hydraulic conductivity estimates in the vicinity of various monitoring wells with a precision that steady-state calibration could not do.

The regional model is highly nonlinear due to the large variability in elevation across the model, thin soil layers over much of the model domain, and the choice of running the model as unconfined. The model would only run using the PCG2 solver (pre-conditioned conjugate gradient method of solving the matrix) with highly damped parameters[3]. Initial solutions that converged required the use of a "rewet" algorithm that is rather crude, but kept the bouncing of predicted head elevations between iterations from zooming out of control. After getting an approximate solution, upland areas of the model were successively turned to no-flow cells where they are predicted to go dry. This damps the solution process further. Eventually the rewet algorithm was turned off and the mass balance error came under control. Once a steady-state solution was obtained, the model was run as a transient solution (but with constant recharge and all other conditions) for 600 days using the calibrated Ss and Sy and average annual precipitation recharge to further minimize the mass balance errors. Figure 4A shows the distribution of no-flow cells put in the top layer of the model and the dry nodes predicted in the steady-state, pre-demo condition, in the vicinity of the site.

[3] The final solution parameters used in the regional model were: Head Change = 0.1; Residual Criterion for Convergence = 0.1; Relaxation Parameter = 1.0; Matrix Preconditioning Method = Polynomial; Maximum Bound on Eigenvalue = computed by program; Damping Factor = 0.5.

One of the complexities encountered during the set up and running of the May and September transient simulations involved varying the river boundary heads with the tide. The CH2M-Hill records for the dock transducer showed the river fluctuating around what was reported as 0.0 feet NGVD. It was also reported that TW-1 water elevations had followed the dock transducer record very closely (same magnitude of tidal fluctuation). The actual determination of River tidal levels is described in Appendix B. It appears that the average annual level of the River is about 1.74 feet, which is what is used in the steady-state simulations. TW-1 is reported to be in surficial deposits screened about 100 feet deep. No reasonable set of hydraulic conductivity and specific storage values can reproduce such a magnitude of response reported for the TW-1 well. This is particularly troublesome because the TW-1 well is quite close to the River and has an average head reported to be a foot or more higher than River level in the spring. It cannot be this close to the River with a head elevated a foot above the River and have the same magnitude of fluctuation. The same situation occurs with MW-108. Given the relatively high average head of MW-108 above River level, it cannot have the measured magnitude of tidal response in combination with the short distance to the discharge canal with any reasonable combination of hydraulic conductivity and specific storage.

Setting up the files for the calibration to the September 2004 pumping test required another set of complex evaluations and corrections to the CH2M-Hill data. Appendix E describes these corrections. There was a large change in barometric pressure during the test, which required corrections to zero out this effect in the wells. CH2M-Hill apparently made some barometric corrections to the data but we elected to do our own. The effects of the tide and recession were included in the model, but the rise due to the barometric drop had to be taken out. Table E-1 present our calculations of barometric efficiency for selected wells. Not all of the monitoring well records were corrected; only those wells most likely to be affected by the pumping well. Therefore, some wells where the records were not corrected show an up-turn at the end of the pumping test in response to barometric drop (we did not carry the simulation beyond the beginning of the heavy rainfall event that occurred in the end of the pumping test).

In the figures illustrating the transient tidal simulations there is an apparent difference in timing between the observed and predicted peaks in groundwater response to high and low tides. The predicted response appears to occur later than (lag) the actual response (comparing peaks and troughs of the tide-influenced curve) by about 1 to 2 hours on most of the records. We believe that we were using Eastern Standard Time uniformly for both the boundary condition transient variation and for the observed heads. The difference in timing is due to the fact that we used a 2-hour time step. Model response to a tide height change would not be recorded until the next time step, two hours later.

We overlaid the CH2M-Hill data for the tide-responsive wells on the same graph as the tide record for May 11-14 (see Figure 16). One can see that there are significant differences among wells in the timing of the peaks and troughs relative to the tide record. Our simulations, however, match the observed peak levels for all wells within an hour except for TW-1 where there is a much greater timing difference, which also shows in Figure 16. We believe that the observed record for TW-1 is invalid for reasons given

above plus the fact that there is such a large lag time between peaks and troughs yet an almost identical magnitude with the River transducer record.

Final mass balance errors for the steady-state, May tide simulation, and September pumping test simulation are given in Tables 4, 5, and 6. The errors are all very low, indicating acceptable accuracy.

GWV produces a standard set of statistics to compare predicted versus observed heads. Tables 7, 8, 9, and 10 contain the statistics for the final calibrated steady-state regional model, steady-state calculated vertical gradients for the site, May tide, and September pumping test simulations. The goal was to keep the standard deviation of residuals divided by head range to ≤ 0.15, which was achieved. We also attempted to keep the difference between predicted and observed heads (called the "residual") to less than one foot. This was achieved with most site monitoring wells. However, there were some exceptions, as noted below:

a) Monitoring wells located in overburden very close to containment were very difficult to match because there was a rock cut around the containment foundation filled with backfill much deeper than the surrounding top of rock. The containment mat sump apparently daylights beyond the edge of the containment foundation wall (as seen in the RHR excavation, for example) but other points of contact with backfilled soil are not known for certain. The narrowness of this trench and the unknown nature of the variability in backfill hydraulic conductivity created complexities beyond the scope of this study. A much finer finite-difference grid and much more detail on the trench topography and soil hydraulic conductivity would be required to match water levels there.
b) Monitoring well MW-104S and several of the shallow 500-series monitoring wells in the parking lot area were apparently located above or partially through an aquitard under the parking lot. This was not confirmed until after the model was designed. It also appears that there may be an unsaturated zone in some areas under this aquitard. Since this model is not capable of simulating saturated-unsaturated conditions (nor are the properties of the site soils--such as variability of hydraulic conductivity with negative pore pressure--known to allow such a simulation), those wells could not be matched. We did include MW-104S in some of the calibrations, however, since there does seem to be some hydraulic connection with the underlying aquifer and there may not be an unsaturated zone under all conditions.
c) Monitoring wells MW-100S, MW-101S, and MW-102S, although designed to monitor shallow bedrock, apparently have screened zones extending above the top of rock. They show rapid rise and fall in water levels during precipitation events. In addition, they are also located just south of the base of a very high and steep hillside where groundwater gradients change drastically over short distances. Since there are no monitoring wells on the hillside above the plant, we can only speculate on the conditions there. The focus with these wells has been more on matching the general direction of vertical gradients.

d) Wells MW-122S and MW-107S are on the edge of a very thick sequence of soils extending east of the containment. Therefore, the hydraulic conductivity here, where soils are 100 feet thick, can be an order of magnitude less than where soils are 10 feet thick and the soil section will still have the same transmissivity. Nonetheless, there are some characteristics of these two wells that we cannot reconcile with the current information. The wells had relatively high levels in the spring and relatively low levels at the end of the summer in 2004, the range of which (compared with the smaller seasonal fluctuation ranges with other site soil wells) implies a relatively low transmissivity. However, the spring high levels were extremely difficult to produce even with very low hydraulic conductivities. Therefore, there must either be an extra source of unknown water to these wells in the spring or there is some type of drainage that lowered the water levels later in the summer. We have simulated the soils east of the containment with a relatively low hydraulic conductivity to attempt to be in the mid-point range of the highs and lows, but this value may be lower than actually exists. This low value may also create the somewhat high predictions of MW-106S and –106D by backing up water that would otherwise drain to the east.
e) The transient simulations need a starting set of heads, which should be a function of the recharge/discharge, and pumping history of the site preceding the simulation period. The site history over the period 2002-2005 is very complicated in terms of when impervious area was removed from certain areas, when certain drains were created or discontinued, and when certain excavations were done and backfilled. We have no local evaporation data. Therefore, trying to determine what the "average groundwater" level is for any well on the site is a difficult task, let alone trying to predict the antecedent recharge/discharge pattern. Nonetheless, we estimated "average head" positions and simulated in a crude way the antecedent recharge/discharge conditions on the site. Although the slope, magnitude, and timing of the predicted tidal response and pumping test response is very close to the observed response in most cases, the spread between observed and predicted heads may be greater than one foot because the starting heads are off by more than one foot.

The average head positions were first estimated by comparison with long-term records of the USGS Connecticut wells in till, bedrock, and sand and gravel where the 1999-2004 record of site wells could be compared with the USGS wells and an average position was found by proportioning. Some adjustments were then made for individual wells to account for effects of site-specific activities such as the nearby presence of dewatering wells.

Figure 17 shows the individual precipitation events and cumulative precipitation for 2004 at the site. Figure B-3 (Appendix B) shows River levels over the same time period. The antecedent simulation was done by starting with the "average annual heads" starting November 2003, then simulating 60 days of five times the average recharge rates (the fall recharge event), then 60 days of no recharge (winter freeze), then 80 days of triple the

average recharge rate (spring recharge event) into the mid-May simulation. This pattern of recharge generally produced the correct water levels at the site through this time span. A severe drought affected the plant region in 2002. Water levels were recovering in 2003. The period from September through December 2003 saw 19.2 inches of precipitation versus a long-time average of 14.2 inches at Bridgeport for the same months. There was significant recovery in site wells during the fall 2003 time frame—much more than normal. Some of this recovery may have been aided by removal of impervious cover associated with decommissioning activities. Spring 2004 recharge was close to the long-term average. Wilson[4] describes the typical pattern of recharge near Worcester, MA, as being distributed in the following pattern: 8% of total recharge occurs in January; 24% of total recharge occurs in February; 36% of total recharge occurs in March; 24% of total recharge occurs in April; and 8% of total recharge occurs in May with none during the rest of the calendar year. The recharge that occurs during any particular time frame is a complex function of antecedent moisture conditions, temperature conditions, snow cover, rainfall intensity and other factors that we have not attempted to address in detail here.

For the September pumping test, we assumed no recharge from mid-May up to the time of the pumping test. Obviously, a more precise accounting for evapo-transpiration and individual large summer rainfall events would improve these starting heads.

6.1 Discussion of Calibration Results

We have evaluated a very large number of possible combinations of aquifer parameters with automated sensitivity runs and individual localized changes of properties in the Kxy, Kz, and leakance categories and many combinations of placement of theoretical lineaments. Standard auto-calibration runs using the Groundwater Vistas routine that vary properties by aquifer property zones were able to reduce errors, but at the expense of going outside of the current conceptual models. Groundwater Vistas calibration procedure employs Marquardt's modification to the Gauss-Newton nonlinear least-squares parameter estimation technique. Given the rather sparse density of monitoring wells, auto-calibration is not capable of moving around narrow linears that were the primary tool of creating agreement in vertical gradients and connecting wells that responded sympathetically to perturbations in head.

The main feature of the regional model calibration with the inclusion of the offsite well data is that the offsite data are overpredicted (predicted heads on average are slightly higher than observed heads). The model was optimized to match the site data. Given that a number of thin linears were added to the bedrock aquifer on the site but none were added away from the site, it would be logical to over-predict offsite levels because there must be a number of linears present in offsite areas, which, if added, would lower water levels in that area.

[4] Wilson, J.L., 1981, Analytical Methods in Groundwater Hydrology, BSCES-ASCE Geotechnical Lecture Series for 1981, Groundwater Hydrology, 116 p.

Figure 18 shows that, for the large range in head over the model area, the match between measured and predicted groundwater heads is good, as reflected in the weighted calibration statistics (Table 7). Residual standard deviation divided by range of head is 0.02 compared with an acceptable upper limit of 0.15. Group 1 heads are the weighted heads from poorly located offsite wells with only one groundwater measurement. Group 2 heads are onsite monitoring wells with many observation points in time. Figure 19 is the same information plotted in a different way with residual plotted on the Y-axis. Although the Group 2 data are tightly clustered around the 0' residual line, the weighted offsite data has some scatter with the majority of points lying in the negative residual range (the model predicts the heads to be greater than measured). This is also illustrated by the mean residual in Table 7 of –4.9'.

Table 8 shows the comparison of measured versus predicted vertical gradients by the steady-state regional model. For reasons described above, we could not match the MW-103 gradient. Except for the MW-122 predicted gradient which is in the right direction, but somewhat weaker than observed, the rest of the gradient predictions are generally good.

Figure 20 shows the comparison of model-predicted heads for the May 2004 tidal simulation with the measured heads during that time frame. As shown in Table 9, there is little vertical bias in the data as the residual mean is essentially zero. Even with all of the difficulties of establishing starting heads and matching storativities and hydraulic conductivities, we had a respectable residual standard deviation divided by range of 0.12.

Figure 21 shows the comparison of model-predicted heads for the September 2004 pumping test simulation with the measured heads during that time frame. As shown in Figure 10, heads are slightly overpredicted (0.54' mean residual), but the residual standard deviation divided by range is still at our limit of 0.15. Obtaining starting heads for the September 2004 pumping test was even more difficult than establishing the May starting heads, yet we still seemed to be in the right range.

The set of Figures 22a-q shows the actual measured water levels during the May 2004 tide simulation compared with the computer-predicted levels for most of the site monitoring wells. Both the May and September 2004 transient simulations show some irregularities in the early part of the predicted record as the simulation shifts from a set of constant boundary conditions and a set of "initial heads" to a transient simulation with varying boundary conditions. The adjustment generally occurs within a day. After the period of adjustment, the overall slope of the measured versus predicted records agree very well, indicating the combination of storativity and transmissivity is good. The spread between observed and predicted is due mostly to the selection of initial heads. The magnitudes of the tidal responses also agree very well except for MW-108 and TW-1, as discussed above. The slight difference in timing between observed versus predicted tidal peaks and troughs are due to the use of 2-hour time steps for the transient simulation.

The set of Figures 23a-s show the actual measured water levels for the September 2004 pumping test simulation, as corrected by Appendix E for barometric changes, compared with the computer-predicted levels for many of the site monitoring wells. As with the May tide simulation, the general slopes of the recession agree very well for most wells. MW-103S was predicted to be rising, so the initial water level for that well was probably not stable at the start of the simulation; we previously described this well as a very difficult well to match. MW-104S was predicted to be declining slower than observed, probably related to the perched nature of the aquifer partially measured by this well. The magnitudes of the tidal responses compared nicely except for TW-1 and MW-108 (previously discussed). The actual responses of MW-110S and MW-113S (not corrected for barometric rise) showed some rise at the last data point, reflecting the large drop in barometric pressure. OB-25, the closest well to the AT-1 pumping well, had observed drawdown at a slower rate than predicted. This may be due to very localized variability in transmissivity or the coarse model grid discretization near the pumping well. Although the finite-difference mesh density was increased around the well, there are still only 2 cell widths between the pumping well and OB-25. Other wells at greater distance such as MW-508 and MW-124 had reasonably good matches with computed drawdown.

6.2 Discussion of Sensitivity Analyses

Even very good calibration of a groundwater model does not mean that all of the properties are correctly spatially defined as there are many combinations of variables that can produce similar point predictions. The sparser the data set, the less unique the solution if it is based on water level matches alone. The systematic variation of individual parameter values above and below the calibrated value gives a good indication of which variables are the most important to the calibration. We have performed sensitivity analyses on recharge rates, horizontal hydraulic conductivity, vertical hydraulic conductivity, bedrock horizontal hydraulic conductivity anisotropy, till leakance, specific yield of soil, and specific storage of bedrock. There are insufficient data to permit calibration of porosity and dispersivity.

Parameter zones were chosen for sensitivity analysis if the zones covered a large area of the model or the zone had multiple site monitoring wells. The sum of squared residuals (RSS) is graphed on the Y-axis as it usually is the most sensitive calibration statistic with the widest range in this type of analysis. The parameter multiplier is given on the X-axis. The parameter multiplier is what is multiplied by the value used in the calibrated model: 1.0 equates to the value used in the calibrated model. Ideally, the RSS would be lowest at a parameter multiplier of 1.0 and be higher for parameter multipliers that would be either higher or lower.

Many of the sensitivity analyses show Type I Sensitivity as defined by ASTM D 5611, meaning that variation of an input causes insignificant changes in calibration residuals as well as the model's conclusions. During the calibration process we generally modified parameters if Type II Sensitivity was indicated, even though changes may have produced little change in model conclusions. Some of the sensitivity analyses show Type III Sensitivity where variation of an input causes significant changes to both the calibration

residuals and to the model's conclusions and parameters were generally modified, unless otherwise noted, to minimize error. We generally have not formally investigated Type IV Sensitivity where the change in calibration residuals is insignificant but the change in the model's conclusions would be significant. However, the extensive trial and error process used to build this model provided the opportunity to try many individual and combinations of changes of parameters and that Type IV Sensitivity of at least the flow model parameters has been vetted fairly thoroughly.

6.2.1 Precipitation Recharge Rate Sensitivity

Figures 24a-e show the sensitivity of the RSS to varying the values of the major precipitation recharge zones. The sensitivity rises rapidly as the rates increased. Above about the 50% of precipitation rate, the recharge rates would go beyond what could be physically achieved except in localized areas where runoff is concentrated and infiltrated. These analyses suggest that the RSS could be reduced by decreasing recharge rate for Zones 2, 3, 4, and 11. This would be logical since the overall steady-state calibration statistic shows that the heads are overpredicted. Therefore, decreasing recharge would result in heads decreasing. As previously explained, head matching was optimized for the site area and a number of bedrock linears were placed within the larger areas of lower transmissivity rock in the site area. If linears were placed throughout the model area, this would lower heads overall.

6.2.2 Horizontal Hydraulic Conductivity Sensitivity

The hydraulic conductivity was simultaneously increased in the same proportion in both the X- and Y-directions. Figures 25a-l summarize the Kxy analyses. These show a variety of responses. Varying the Kxy of Zones 3, 14, 21, 24, 25, 29, 33, and 40 shows very small sensitivity. Zone 1 (the predominant rock zone in layers 5, 6, 7, and 8) is the most sensitive as shown in Figure 25a. The sensitivity of zones 17 (predominant rock in layer 4) and 18 (predominant rock in layer 9) suggest that calibration could be improved slightly by increasing the Kxy of those zones.

6.2.3 Vertical Hydraulic Conductivity Sensitivity

Vertical hydraulic conductivity (Kz) is one of the least sensitive variables overall as shown in Figures 26a-g.

6.2.4 Bedrock Horizontal Hydraulic Conductivity Anisotropy Ratio Sensitivity

Groundwater Vistas does not have an automated routine to perform sensitivity analyses on some of the variables such as anisotropy. Figure 27 shows our analysis and that the variable has very low sensitivity to anisotropy ratios of Ky/Kx from 0.5 to 5. We have used a modest anisotropy ratio of 2 in the model to incorporate field observations of the prominent north-south foliation fabric. This is part of the conceptual model formulated by CH2M-Hill and one that we generally agree with based on our observations of the rock and experience in similar geologic terrain.

6.2.5 Till Leakance Sensitivity

The model simulates an aquitard layer between layers 3 and 4 to represent the thin till layer that has been found in many site borings. The thickness of this layer is represented by the difference between the elevation of the bottom of layer 3 and the top of layer 4, which is almost everywhere represented as one foot thick in the model. This pseudo layer is represented by a leakance or a resistance to vertical flow across the layer boundary. The leakance (K'/B) is a moderately sensitive variable as shown in Figure 28. If the till layer is removed or the leakance is increased somewhat, calibration error goes up quickly. The thickness and porosity of this pseudo layer is an input and accounted for in MODPATH to keep the particle tracking routine in a manner to correctly represent the till layer.

6.2.6 Sensitivity of Specific Yield of Soil Layers

The two transient simulations required the calibration of specific yield and specific storage. Results were not very sensitive to specific yield as shown on Figure 29.

6.2.7 Sensitivity of Specific Storativity of Bedrock

The specific storativity of the bedrock is a somewhat more sensitive variable than the soil specific yield and Figure 30 suggests that if storativity was increased that calibration would be improved slightly. Increasing storativity damps the response of perturbations in boundary conditions such that, for example, the range of tidal response would decrease. Since we have achieved relatively good matches with the range of tidal response and with the slope of the recession curves, and since we tried many combinations of storativity during calibration, we believe that we have the right value for most of the site aquifer.

7 Specific Simulations

Figures 31 through 53 were all created from TMR submodels of the regional models. All TMR models were created by fixing the heads in boundary cells around the edge of the TMR model. For runs that involved transient scenarios such as a dewatering or rewetting scenario, the TMR boundary heads would usually change with each time step and were established by first simulating the transient flow condition in the regional model and capturing the heads at each TMR boundary cell for each time step and passing those heads through to the TMR model for the same time step. Theoretically, the flow model within the domain of a TMR model should be identical to the flow domain within the same area of the regional model. The TMR model is just a more efficient way to execute a model run faster and provide more detail in the output compared with the regional model. Groundwater Vistas provides a very convenient routine of creating a new submodel out of a larger model, preserving all properties, boundary conditions and layering. Even a finer grid mesh is created, this process is usually seamless, although some minor adjustments are made to get more local detail when larger cells become

smaller cells, such as in decreasing the apparent area covered by a "drain" boundary condition cell.

7.1 Reverse Particle Tracking with the Steady-state Operational Condition

Figures 31, 32, 33, and 34 show the groundwater heads predicted by the steady-state pre-demolition condition model for model layers 1, 4, 6, and 8. The cone of depression around containment from the foundation sump and foundation mat drains is clearly shown in the soil layers and the top rock layer. A localized groundwater divide is created under the turbine building in all layers down to model layer 6. This could create some localized but deep penetration into the bedrock of contaminants that might have entered the aquifer under this groundwater divide. Figures 33 and 34 show the effects of linears that were placed in the model.

Figure 35 shows the results of reverse particle tracking from some of the monitoring wells on the site that have shown radionuclide concentrations above background at some time in their history. The particle traces are color-coded to show which model layer they are traveling in each point in the travel path. The linears placed in the model tend to collect groundwater traces and focus them along north to south flow lines. These linears have been shown by field studies such as packer test responses and continuity of radioactive and boron plumes to be the major controls on the site. Wells MW-124, -118, -121, and –110 are located on a pathway that leads northward under the containment. The paths of wells MW107 and –122 lead under tanks located east of the spent fuel pool. Well 105 lies directly on a line with flow from the PAB and RHR pit. It is possible that MW-104 could be on a flow line from the tank farm. Solute transport simulations involving the use of finite dispersivities shows the type of spreading that one would expect in the real world, but with the centerline of the contaminant plumes focused by the linears.

7.2 Flow Simulations and Particle Tracking under Maximum Dewatering Conditions

Figures 36, 37, 38, and 39 show predicted groundwater heads during steady-state conditions of maximum dewatering of the site under average annual recharge conditions. This might approximate conditions in the spring of 2005 when the RHR pit and PAB excavation were open. The pattern of contours is similar to the operational condition except that several more small localized groundwater divides appear.

Figure 40 shows the results of forward particle tracking from two lines of points in layers 3 and 4. One particle source line runs east-southeast through the tank farm and spent fuel pool. The second lines runs just north of the discharge tunnel. Figure 40 shows capture of flow to the west of the tank farm in the dewatering just under the tank farm. From east of the tank farm to the east end of the tanks east of the spent fuel pool, the containment foundation sump captures the flow. Particles originating on the east end of the northerly line of particle sources pass south through the MW-122 area and on to the discharge canal. Particles started near MW-105 flow north to be intercepted by dewatering next to the cable vault. Source points on the west end of the discharge tunnel flow west then

south around the tunnel wall. Sources points on the east end of the discharge tunnel flow east around the east end of the tunnel, then southwest.

7.3 Post Demolition Conditions

Figures 41, 42, 43, and 44 show the simulated heads at the site in the post demolition under average annual recharge conditions. These simulations suggest that a local groundwater divide will still occur under the former turbine building. Groundwater flow in the soil and top rock layer will be generally south-southwest through containment to the River with heads dropping off to both east and west where soil is thicker.

Figure 45 shows forward particle tracks from two rows of arbitrary source points in model layers 3 and 4. These particle source points are similar to those in Figure 40. This simulation suggests that sources under the Tank Farm, RHR, PAB and area north of the discharge tunnel and east of MW-105 will flow west and then south. Areas under containment will flow south through MW-106 and around the end of the discharge tunnel before turning to flow south-southwest. The spent fuel building particle sources flow through the area of MW-107. From the tanks north of MW-122, flow goes south through MW-122, across the discharge canal and then southwest to pass between MW-110 and MW-111.

7.3.1 Conditions During a Post-demo 60-day Dewatering under the Spent Fuel Pool

Two post-demolition construction scenarios were simulated to see what effect temporary dewatering might have on flow paths. The first simulation assumes that the area under the spent fuel pool is dewatered to elevation –2' NGVD. Figures 46, 47, and 48 show the heads in layers 1, 4, and 6 at the end of 60 days of dewatering under average annual recharge conditions. These show the prominent localized effect of the dewatering and a strong groundwater divide developed under the area of the former turbine building.

Figure 49 shows forward particle tracking with particles started in three lines across the IA in layers 3 and 4. The capture zone lies close to and mostly north of the spent fuel building. Sixty days is not enough time to induce flow into the pit except from a small area in the eastern half of the containment.

7.3.2 Conditions During a Post-demo 60-day Dewatering along the northern edge of the Discharge Tunnel

This final set of post-demo construction scenarios involves dewatering the trench on the north side of the discharge tunnel to –2' NGVD for 60 days. Figures 50, 51, and 52 show the heads in layers 1, 4, and 6 at the end of 60 days of dewatering starting with average annual conditions. The head contours show that flow from both directly north and south would be captured in the dewatering system. Figure 53 shows forward particle tracking from a line of source points running east-southeast through the former tank farm and spent fuel pool. A source starting from the MW-103 area might make it to the dewatered trench in 60 days, but otherwise the flow pattern from the north is little affected.

8 Summary

A regional 3-D groundwater flow model based on MODFLOW96, as implemented in Groundwater Vistas GW4.18, has been constructed to include the Connecticut Yankee Nuclear Plant site. This model covers a large area on both sides of the Connecticut River so that the model boundaries are naturally located on streams and groundwater divides far from the nuclear plant site. The finite-difference grid cells are discretized with variable spacing from 6.5 feet near the center of the plant site to as far apart as 510 feet near the outer limits of the model. The steady-state calibration model used minimum cell widths of 25 feet, whereas the transient model used to verify the September 2004 pumping test used the smaller grid spacing of 6.5 feet near the pumping well. The model consists of 9 layers: 3 soil layers and 6 bedrock layers. The model extends 600 feet into bedrock with layer thicknesses increasing with depth. All of the top 7 layers of the model were permitted to perform as unconfined layers if the layers above were dewatered by the simulation.

MODFLOW, MODPATH (used for particle tracking), and MT3DMS (used for solute transport simulations) are porous media models. Appendix A to the report describes our defense of using porous media models to simulate flow and transport in fractured bedrock.

A large variety of data sources were utilized to parameterize the model. These sources were obtained either through the State of Connecticut GIS database, or from CH2M-Hill. These sources were pre-processed with Rockware, Surfer, and ArcView software. We utilized 94 locations with measured water levels from a variety of depths and geologic units as calibration targets for the regional steady-state model. We conducted two transient simulations for calibration purposes: varying adjusted measured tidal levels May 13-15, 2004; and, pumping well AT-1 and varying adjusted measured tidal levels September 15-17, 2004. Continuously recorded onsite transducer measurements in 20 monitoring wells were used to calibrate the May tide simulation model; 22 monitoring wells were used to calibrate the September pumping test. We also used measured vertical groundwater gradients from 9 onsite paired wells to match vertical gradients measured on the site.

The calibration goals were to achieve a standard deviation of residuals (observed versus predicted levels) divided by the range of measured values (highest value minus lowest value) of ≤ 0.15 and to keep the difference between onsite measured levels and predicted levels to less than one foot. The first goal was achieved in all cases; there were some exceptions to the second goal as explained in detail in the report. Overall, considering the highly non-linear nature of the model, the fact that we were simulating fractured bedrock aquifers, the unknown permeability distribution of site fill, and the sharp permeability transitions around containment and the foot of the cliff to the north, the models performed very well in matching observed steady-state levels, recession following recharge events, pumping stresses, and varying Connecticut River levels. Mass balance errors for all final simulations were very low.

We performed a large number of sensitivity analyses to illustrate the sensitivity of major model variables to varying the parameter through a reasonable range. These results are displayed graphically and discussed in the report.

Although not described in detail in this report, the model has been used for solute transport simulations involving potential bedrock contamination under the tank farm. The derivation of the parameters involved in transport simulations of radioactive constituents is described in Appendix D of the report.

The groundwater contours and particle tracking are presented from a number of scenarios that were simulated. We present reverse particle tracking from many site monitoring wells under the average conditions that probably existed during plant operations. We show predicted groundwater contours at various depths and particle tracking during the maximum dewatering conditions that occurred in the spring of 2005. We show the predicted post-demolition groundwater heads and particle tracking for the future average condition. We present groundwater heads and particle tracking from a hypothetical 60-day dewatering and excavation of the spent fuel pool down to –2' NGVD to show how heads and flow paths would be modified in the vicinity of the excavation. We also show groundwater heads and particle tracking from a hypothetical 60-day dewatering and excavation of soil to –2' NGVD along the north side of the discharge tunnel, again to show how heads and flow paths would be modified during such an excavation.

The model has reproduced reasonably well the measured groundwater contour patterns over the site during various seasons and dewatering conditions. The flow paths and solute transport simulations that have been performed also appear to conform to the known pathways of contaminants that have moved across the site from known source areas. The model should be a useful tool in predictive analysis.

Table 1
Hydraulic Conductivity Values
CY Groundwater Model

Zone	Kx, ft/day	Ky, ft/day	Kz, ft/day	Where Applied?
1	7.50E-02	1.50E-01	1.50E-02	layers 5-8 rock in most of model
2	5.00E-02	5.00E-02	5.01E-02	not used
3	4.50E-02	9.00E-02	2.70E-02	fol amph west of contain. Lyr 4
4	5.03E-02	5.03E-02	5.03E-02	not used
5	5.04E-02	5.04E-02	5.04E-02	not used
6	5.05E-02	5.05E-02	5.00E-02	schist west of amph. At site
7	4.91E-02	4.91E-02	4.91E-02	not used
8	4.92E-02	4.92E-02	4.92E-02	not used
9	4.93E-02	4.93E-02	4.93E-02	not used
10	4.94E-02	4.94E-02	4.94E-02	not used
11	4.95E-02	4.95E-02	4.95E-02	not used
12	4.96E-02	4.96E-02	4.96E-02	not used
13	5.00E-03	5.00E-03	5.00E-03	mylonite zone
14	1.00E+01	1.00E+01	1.00E+01	western-most high perm linear
15	1.01E-01	1.01E-01	1.01E-01	not used
16	4.97E-02	4.97E-02	4.97E-02	not used
17	2.50E-02	5.00E-02	1.50E-02	top rock layer in most of model
18	7.50E-03	1.50E-02	1.50E-02	layer 9 rock in most of model
19	1.00E-01	1.00E-01	3.00E+00	not used
20	5.00E+01	5.00E+01	5.00E+00	sand and gravel
21	1.00E+01	1.00E+01	1.00E+00	red fine sand; also some fill
22	5.00E-01	5.00E-01	5.00E-02	till
23	5.00E-01	5.00E-01	1.00E-01	till
24	1.00E+01	1.00E+01	4.00E-01	clay-silt and peat
25	1.09E-01	1.09E-01	1.05E-01	thick lodgment till
26	3.00E-01	3.00E-01	1.00E-01	thick sandy till
27	3.00E-03	6.00E-03	6.00E-03	transitional rock lyr 4-8 N of plant
28	2.50E+01	2.50E+01	1.00E+01	sand & gr north half parking lot
29	3.00E+01	3.00E+01	3.00E+01	easternmost linear through B110
30	5.00E-01	5.00E-01	5.00E-02	till/fill on north edge of plant grade
31	5.00E+00	5.00E+00	5.00E+00	frac zone w/ springs above plant
32	1.00E+02	1.00E+02	2.00E+01	s&g extending north thru AT-1
33	3.00E+00	3.00E+00	3.00E+00	linear through MW106
34	3.00E-01	3.00E-01	1.00E-01	not used
35	1.00E-01	1.00E-01	1.00E-02	not used
36	1.00E-01	1.00E-01	1.00E-01	not used
37	1.50E-01	3.00E-01	3.00E-01	high hor. K zone layer 5 at plant
38	3.00E+01	3.00E+01	3.00E+01	linear through MW101
39	3.00E+00	3.00E+00	3.00E+00	N60E linear thru MW102 lyr 5
40	2.00E-01	2.00E-01	2.00E-02	low K soil zones in plant area
41	1.00E-01	1.00E-01	1.00E-01	N60E linear thru MW102 lyr 4

Table 2
Average Annual Precipitation Recharge Rate
CY Groundwater Model

Zone	Recharge Rate, ft/day	Applied Where?
1	0.0000	not used
2	0.0036	sandy till
3	0.0024	thin soils and exposed rock
4	0.0027	thick lodgment till
5	0.0014	clay-silt
6	0.0050	surface water
7	0.0002	paved area
8	0.0000	roofs and impervious area
9	0.0370	leachfield (includes disposal rate)
10	0.0050	soils at north edge of plant under cliff
11	0.0046	sand and gravel
12	0.0000	not used

Table 3
Specific Storage, Specific Yield, and Effective Porosity
CY Groundwater Model

Zone	Specific Storage	Specific Yield	Effective Porosity	Where Applied?
1	1.00E-05	0.3000	0.2500	most soils
2	3.00E-06	0.0100	0.0120	most bedrock
3	1.00E-07	0.0300	0.3000	soils layer 2, west of plant
4	3.00E-05	0.0100	0.0120	around MW103 lyr 3&4
5	1.00E-04	0.1000	0.3000	not used
6	3.00E-06	0.0010	0.0010	not used
7	3.00E-05	0.0100	0.0010	not used
8	3.00E-06	0.0001	0.0001	not used

Table 4
Steady-State Model Mass Balance Summary
CY Groundwater Model

Description	Inflow (ft3/day)	Outflow (ft3/day)
Recharge	1.09E+06	0.00E+00
Constant Head	3.12E+03	3.46E+05
Drain	0.00E+00	7.58E+05
GHB	7.63E+03	6.82E+01
Well	0.00E+00	1.20E+03
Storage	0.00E+00	0.00E+00
TOTAL	**1.10E+06**	**1.10E+06**
ERROR	***1.58E-02***	***%***

Containment Foundation Sump Ave. Flow = 684 ft3/day

Table 5
May 2004 Tide Simulation Mass Balance
CY Groundwater Model

Description	Inflow, ft3/day	Outflow, ft3/day
Recharge	3.70E+05	0.00E+00
ET	0.00E+00	0.00E+00
Constant Head	1.24E+06	1.10E+05
River	0.00E+00	0.00E+00
Lake	0.00E+00	0.00E+00
Drain	0.00E+00	1.46E+06
GHB	7.71E+03	8.21E+02
Well	0.00E+00	1.20E+03
Stream	0.00E+00	0.00E+00
Storage	1.63E+06	1.67E+06
TOTAL	**3.25E+06**	**3.25E+06**
ERROR	**-2.02E-04**	**%**

Table 6
Mass Balance for September 2004 Pumping Test Simulation
CY Groundwater Model

Description	Inflow in ft3/day	Outflow in ft3/day
Recharge	9.76E+02	0.00E+00
ET	0.00E+00	0.00E+00
Constant Head	0.00E+00	1.58E+06
River	0.00E+00	0.00E+00
Lake	0.00E+00	0.00E+00
Drain	0.00E+00	4.26E+05
GHB	8.67E+03	1.80E+00
Well	0.00E+00	6.79E+03
Stream	0.00E+00	0.00E+00
Storage	2.00E+06	4.29E+03
TOTAL	**2.01E+06**	**2.01E+06**
ERROR	**-1.65E-04**	**%**

Table 7
Steady-State Calibration Statistics
CY Groundwater Model

Name	Layer	Observed Head (feet)	Computed Head (feet)	Weight	Group	Residual
CYR32	9	68	121.93	0.2	1	-10.79
MW-107S	1	5.14	4.79	1	2	0.35
MW-124	3	3	2.79	1	2	0.21
MW-508D	4	4.35	3.94	1	2	0.41
EHP398	5	422	451.48	0.2	1	-5.90
H19	3	2	2.55	0.2	1	-0.11
H23	4	7	4.63	0.2	2	0.47
H413	6	47	137.26	0.2	1	-18.05
H421	3	11	8.22	0.2	1	0.56
H426	7	220	187.06	0.2	1	6.59
H428	8	66	103.04	0.2	1	-7.41
H429	8	130	148.79	0.2	1	-3.76
H430	7	220	233.87	0.2	1	-2.77
H431	9	82	110.32	0.2	1	-5.66
H435	6	67	121.69	0.2	1	-10.94
H437	7	379	445.30	0.2	1	-13.26
H439	3	2	2.54	0.2	1	-0.11
H440	6	27	78.76	0.2	1	-10.35
H443	7	321	357.49	0.2	1	-7.30
H444	4	32	7.27	0.2	1	4.95
H445	6	335	361.09	0.2	1	-5.22
H446	8	75	113.10	0.2	1	-7.62
H447	5	184	243.77	0.2	1	-11.95
H451	7	135	131.52	0.2	1	0.70
H452	8	160	184.70	0.2	1	-4.94
H456	7	79	131.74	0.2	1	-10.55
H458	6	153	200.99	0.2	1	-9.60
CYR1	6	58	93.81	0.2	1	-7.16
CYR2	9	357	335.86	0.2	1	4.23
CYR3	7	282	305.60	0.2	1	-4.72
CYR7	9	54	182.93	0.2	1	-25.79
CYR8	9	90	190.58	0.2	1	-20.12
CYR9	9	337	380.50	0.2	1	-8.70
CYR10	9	346	380.84	0.2	1	-6.97
CYR11	7	392	445.55	0.2	1	-10.71
CYR12A	9	372	411.95	0.2	1	-7.99
CYR15	9	52	180.55	0.2	1	-25.71
CYR17	9	106	175.44	0.2	1	-13.89
CYR19	6	11	75.29	0.2	1	-12.86
CYR28	8	11	99.88	0.2	1	-17.78
CYR33	9	80	127.53	0.2	1	-9.51
CYR34	9	108	132.52	0.2	1	-4.90
CYR37	9	95	140.27	0.2	1	-9.05
CYR41	9	10	99.00	0.2	1	-17.80
CYR42	7	113	97.97	0.2	1	3.01

Table 7
Steady-State Calibration Statistics
CY Groundwater Model

Name	Layer	Observed Head (feet)	Computed Head (feet)	Weight	Group	Residual
CYR43	8	102	95.62	0.2	1	1.28
CYR44	7	51	97.55	0.2	1	-9.31
CYR46	8	65	82.03	0.2	1	-3.41
CYR48	8	47	49.39	0.2	1	-0.48
CYR49	6	59	88.04	0.2	1	-5.81
CYR50	7	66	100.75	0.2	1	-6.95
CYR51	9	58	111.22	0.2	1	-10.64
CYR52	6	134	161.60	0.2	1	-5.52
CYR53	9	185	208.55	0.2	1	-4.71
CYR54	8	79	107.04	0.2	1	-5.61
CYR56	6	56	91.84	0.2	1	-7.17
CYR57	8	54	95.92	0.2	1	-8.38
CYR58	8	70	99.92	0.2	1	-5.98
CYR59	6	83	106.14	0.2	1	-4.63
CYR61	7	161	190.91	0.2	1	-5.98
CYR62	9	97	125.71	0.2	1	-5.74
CYR63	6	158	156.67	0.2	1	0.27
CYR64	9	101	119.03	0.2	1	-3.61
CYR65	7	281	210.88	0.2	1	14.02
CYR68	8	69	137.61	0.2	1	-13.72
CYR70	9	190	247.06	0.2	1	-11.41
CYR71	6	97	164.74	0.2	1	-13.55
CYR73	7	85	147.70	0.2	1	-12.54
CYR75	9	70	115.55	0.2	1	-9.11
CYR77	7	92	125.01	0.2	1	-6.60
CYR79	8	89	89.93	0.2	1	-0.19
CYR80	7	85	101.31	0.2	1	-3.26
CYR81	9	79	89.37	0.2	1	-2.07
MW-100S	3	14	15.00	1	2	-1.00
MW-104S	3	10.83	8.30	1	2	2.53
MW-108	1	4	4.85	1	2	-0.85
MW-109S	3	2.92	2.25	1	2	0.67
MW-110S	1	2	1.89	1	2	0.11
MW-113S	1	2.58	1.81	1	2	0.77
MW-114S	3	6	5.14	1	2	0.86
MW-122S	1	7.04	8.36	1	2	-1.32
MW-504	2	4	4.23	1	2	-0.23
TW-1	3	1.74	1.80	1	2	-0.06
MW-102D	5	8.19	7.97	1	2	0.22
MW-103D	5	6	6.71	1	2	-0.71
MW-106D	5	6.85	6.17	1	2	0.68
MW-122D	8	4	4.83	1	2	-0.83
MW-101S	4	15.73	11.51	1	2	4.22
MW-102S	4	11.6	9.85	1	2	1.75
MW-103S	4	7	1.93	1	2	5.07

Table 7
Steady-State Calibration Statistics
CY Groundwater Model

Name	Layer	Observed Head (feet)	Computed Head (feet)	Weight	Group	Residual
MW-106S	4	8.77	5.87	1	2	2.90
MW-107D	4	6.44	4.23	1	2	2.21
MW-109D	4	6	4.93	1	2	1.07
MW-110D	4	3	2.98	1	2	0.02

Residual Mean	**-4.91**
Res. Std. Dev.	**6.79**
Sum of Squares	**6600.28**
Abs. Res. Mean	**6.19**
Min. Residual	**-25.79**
Max. Residual	**14.02**
Range	**420.26**
Std/Range	**0.02**

Table 8
Steady-State Vertical Gradient Calibration Results
CY Groundwater Model

Well Pair	Upper Model Layer	Lower Model Layer	Observed Vertical Head Difference in Feet	Computed Vertical Head Difference in Feet	Residual Vertical Head Difference in Feet
MW-101	4	5	5	0.8	4.2
MW-102	4	5	2	1.4	0.6
MW-103	4	5	2	-3.9	5.9
MW-105	3	5	-2	-3.0	1.0
MW-106	4	5	0	-0.1	0.1
MW-107	1	4	0	0.8	-0.8
MW-109	3	4	-3	-3.0	0.0
MW-110	1	4	-1	-1.1	0.1
MW-122	1	8	0.5	4.3	-3.8

Table 9
May Tide Simulation Calibration Statistics
CY Groundwater Model

Name	Time (days)	Layer	Observed Head (ft., NGVD)	Predicted Head (ft. NGVD)	Residual
MW-107S	0.08	1	7.55	4.68	2.87
MW-107S	4.00	1	7.06	4.74	2.32
MW-100S	0.08	3	14.91	16.59	-1.68
MW-100S	4.00	3	14.67	16.18	-1.51
MW-108	0.08	1	5.20	7.94	-2.74
MW-108	4.00	1	5.55	6.47	-0.92
MW-110S	0.08	1	2.01	2.04	-0.03
MW-110S	4.00	1	1.50	1.23	0.27
MW-122S	0.08	1	10.58	5.66	4.92
MW-122S	4.00	1	9.88	5.71	4.17
MW-124	0.08	3	3.86	3.49	0.37
MW-124	4.00	3	3.65	2.86	0.79
MW-504	0.08	2	4.16	4.48	-0.32
MW-504	4.00	2	3.95	4.44	-0.49
TW-1	0.08	1	3.04	1.92	1.12
TW-1	4.00	1	3.81	1.42	2.39
MW-102D	0.08	5	10.08	11.37	-1.29
MW-102D	4.00	5	9.25	11.34	-2.09
MW-103D	0.08	5	11.19	10.94	0.25
MW-103D	4.00	5	10.44	11.07	-0.63
MW-106D	0.08	5	7.94	9.18	-1.24
MW-106D	4.00	5	7.27	9.14	-1.87
MW-122D	0.08	8	5.86	6.33	-0.47
MW-122D	4.00	8	5.32	5.74	-0.42
MW-101S	0.08	4	15.55	15.21	0.34
MW-101S	4.00	4	15.14	12.68	2.46
MW-102S	0.08	4	11.50	13.76	-2.26
MW-102S	4.00	4	11.20	13.05	-1.85
MW-103S	0.08	4	8.96	8.73	0.23
MW-103S	4.00	4	8.29	6.52	1.77
MW-106S	0.08	4	8.06	8.91	-0.85
MW-106S	4.00	4	7.72	8.95	-1.23
MW-107D	0.08	4	7.69	6.27	1.42
MW-107D	4.00	4	7.21	5.37	1.84
MW-109D	0.08	4	4.56	6.49	-1.93
MW-109D	4.00	4	4.37	5.74	-1.37
MW-110D	0.08	4	3.31	3.74	-0.43
MW-110D	4.00	4	3.10	3.17	-0.07
MW-508D	0.08	4	4.07	4.48	-0.41
MW-508D	4.00	4	3.84	4.25	-0.41

Table 9
May Tide Simulation Calibration Statistics
CY Groundwater Model

Residual Mean	0.0002
Res. Std. Dev.	1.79
Sum of Squares	3068.09
Abs. Res. Mean	1.45
Min. Residual	-3.00
Max. Residual	4.92
Range	14.34
Std/Range	0.12

Note: Only the first and last time step of 49 time steps are listed for each well; however, statistics are computed based on all time steps.

Table 10
Calibration Statistics for September 2004 Pumping Test Simulation
CY Groundwater Model

Name	Time in days since 9/15/04 0:00	Model Layer	Corrected Measured Head, ft. NGVD	Model Simulated Head, ft. NGVD	Residual, ft.
MW-107S	0.555	1	2.33	4.60	-2.27
MW-107S	2.333	1	2.23	4.60	-2.37
MW-109S	0.555	3	3.01	2.15	0.85
MW-109S	2.333	3	2.57	1.86	0.71
MW-113S	0.555	1	1.94	1.74	0.20
MW-113S	2.333	1	1.67	1.52	0.15
MW-100S	0.555	3	11.93	13.66	-1.72
MW-100S	2.333	3	11.94	13.62	-1.68
MW-104S	0.555	3	7.83	8.77	-0.93
MW-104S	2.333	3	7.38	8.74	-1.36
MW-108	0.555	1	2.83	3.48	-0.65
MW-108	2.333	1	1.70	3.42	-1.72
MW-110S	0.555	1	2.18	1.64	0.54
MW-110S	2.333	1	1.96	1.57	0.39
MW-124	0.555	3	2.84	2.60	0.24
MW-124	2.333	3	2.25	2.14	0.11
MW-504	0.080	2	4.16	4.12	0.04
MW-504	2.330	2	4.04	4.08	-0.04
TW-1	0.555	1	2.39	1.70	0.69
TW-1	2.333	1	1.75	1.53	0.22
MW-102D	0.555	5	1.33	4.72	-3.39
MW-102D	2.333	5	1.28	5.59	-4.32
MW-103D	0.555	5	3.84	5.81	-1.97
MW-103D	2.333	5	3.72	6.57	-2.86
MW-106D	0.555	5	1.30	5.34	-4.05
MW-106D	2.333	5	1.14	5.72	-4.57
MW-122D	0.555	8	3.71	4.16	-0.44
MW-122D	2.333	8	3.50	4.00	-0.49
MW-101S	0.555	4	13.96	8.02	5.94
MW-101S	2.333	4	13.88	8.15	5.73
MW-106S	0.555	4	2.79	5.13	-2.34
MW-106S	2.333	4	2.86	5.56	-2.70
MW-109D	0.555	4	3.04	4.57	-1.53
MW-109D	2.333	4	2.59	4.35	-1.76
MW-110D	0.555	4	2.12	2.78	-0.66
MW-110D	2.333	4	1.58	2.60	-1.03

Table 10
Calibration Statistics for September 2004 Pumping Test Simulation
CY Groundwater Model

Name	Time in days since 9/15/04 0:00	Model Layer	Corrected Measured Head, ft. NGVD	Model Simulated Head, ft. NGVD	Residual, ft.
MW-508D	0.555	4	3.18	3.76	-0.58
MW-508D	2.333	4	2.64	3.52	-0.88
OB-25	0.555	3	2.70	2.48	0.22
OB-25	2.333	3	1.93	0.93	1.00
MW-123	0.555	4	4.41	5.53	-1.13
MW-123	2.333	4	4.12	5.44	-1.32
MW-103S	0.555	4	1.73	0.18	1.55
MW-103S	2.333	4	1.63	2.12	-0.49

Residual Mean	**-0.54**
Res. Std. Dev.	**1.88**
Sum of Squares	**1149.78**
Abs. Res. Mean	**1.33**
Min. Residual	**-4.57**
Max. Residual	**5.94**
Range	**12.82**
Std/Range	**0.15**

Note: Only the first and last target times for each well are presented above although all of the residuals from all of the time steps were used in calculating the statistics.

CY Regional Groundwater Model Geologic Data Points

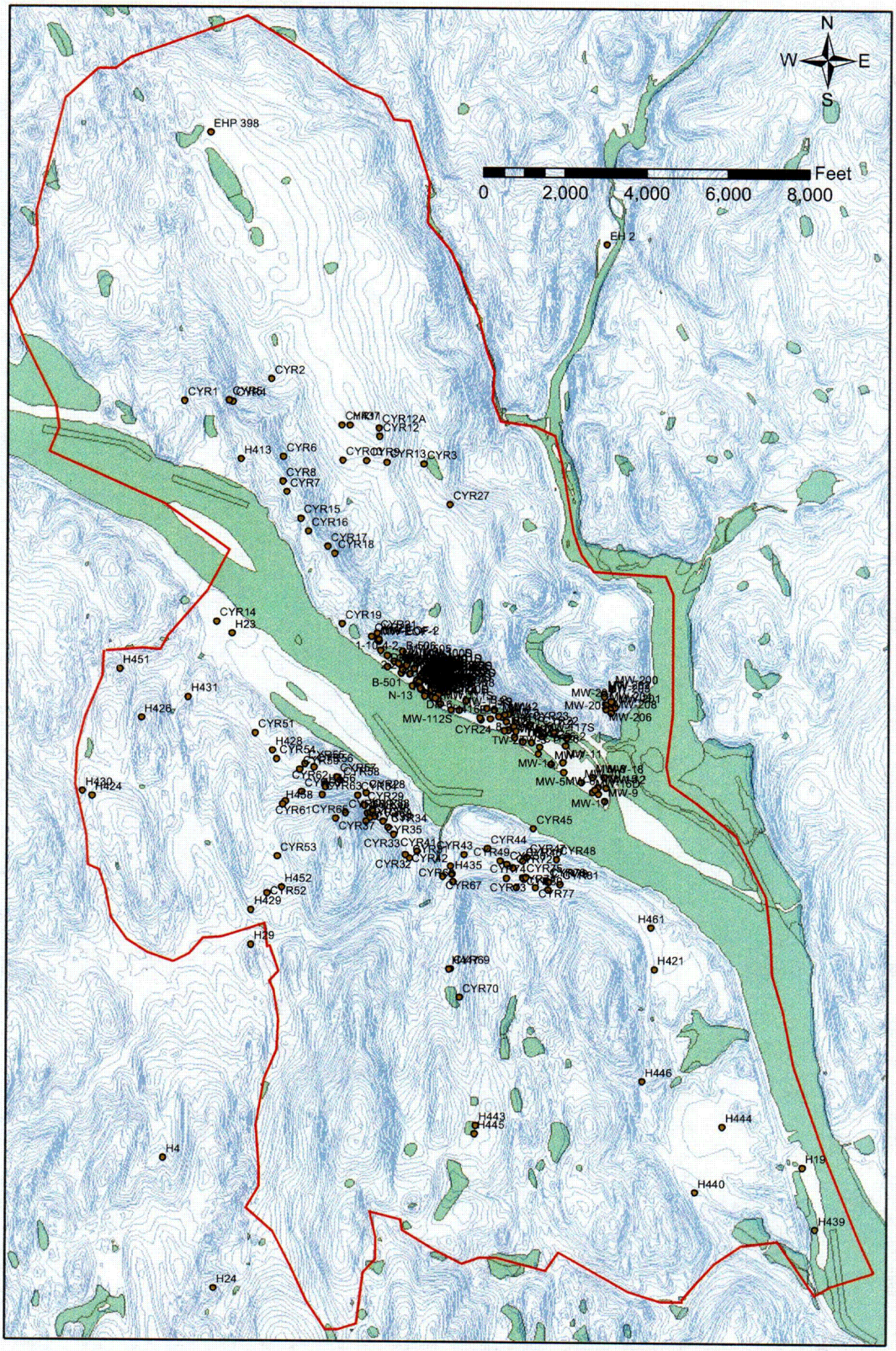

Data sources:
USGS Water Resources reports
Survey of Private Wells by Connecticut Yankee staff
Wells and borings drilled on Connecticut Yankee property

Red line indicates outer boundary of active area of groundwater model

STRATEX
strategic consulting

Figure 1

CY Regional Groundwater Model Top of Rock Elevation

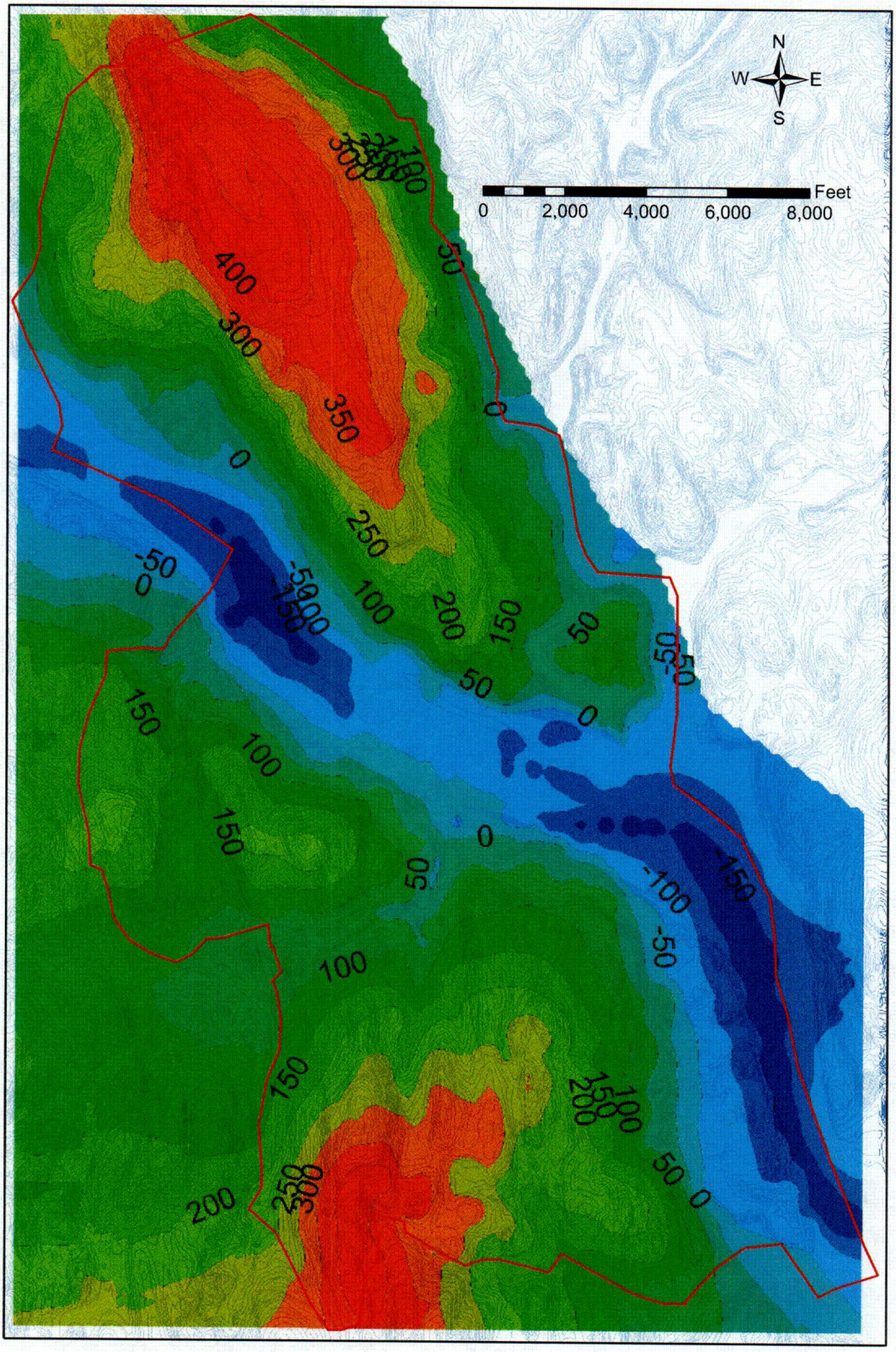

Data sources:
Well and boring data
Surficial Geology Maps (subtract thickness from ground topo)
Soils Maps (subtract thickness from ground topo)

Red line indicates outer boundary of active area of groundwater model

STRATEX
strategic consulting

Figure 2

C02

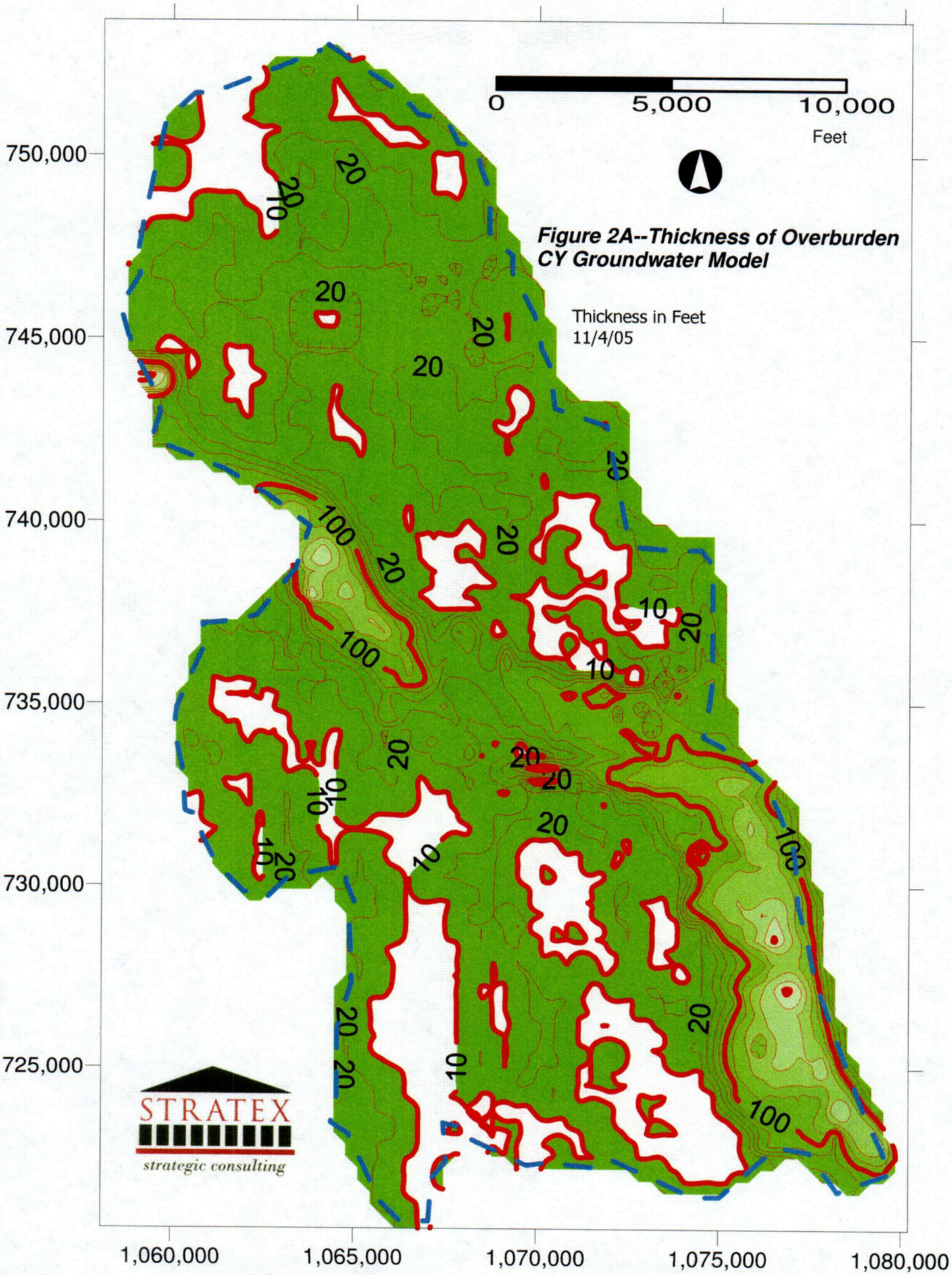
0
5,000
10,000
Feet
Figure 2A--Thickness of Overburden
CY Groundwater Model
Thickness in Feet
11/4/05
750,000
745,000
740,000
735,000
730,000
725,000
1,060,000
1,065,000
1,070,000
1,075,000
1,080,000
STRATEX
strategic consulting

C03

CY Regional Groundwater Model Finite-difference Grid

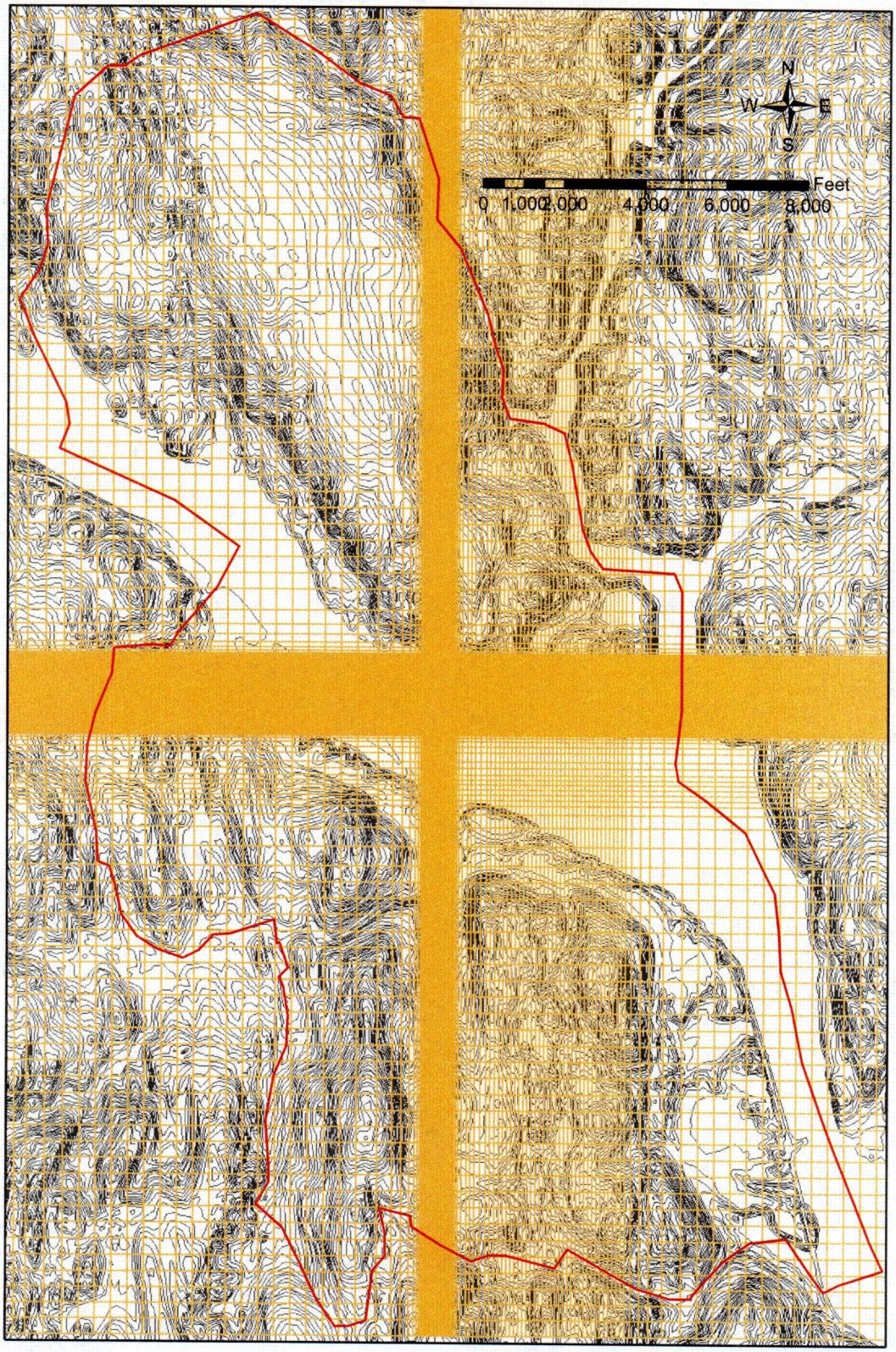

Red line indicates outer boundary of active area of groundwater model
Model has 171 Rows, 124 Columns, and 9 Layers
There are 108285 active cells in the model.
Minimum cell width is 25 feet; maximum cell width is 510 feet.

STRATEX
strategic consulting

Figure 3

C04

CY Regional Groundwater Model Boundary Conditions

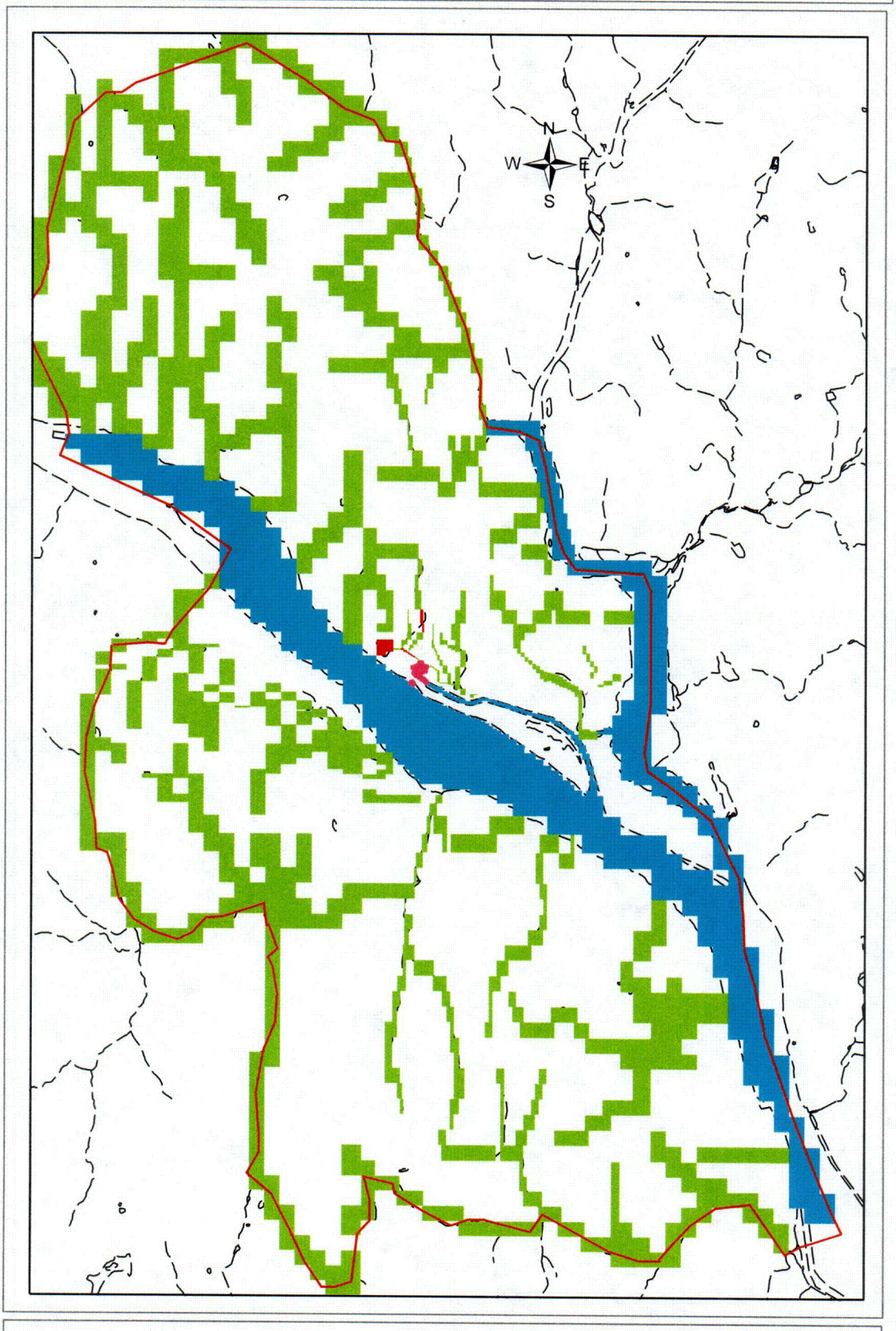

Legend

Constant Head

Drain

Barrier Wall

General Head Boundary

0 2,100 4,200 6,300 8,400 Feet

STRATEX
strategic consulting

Figure 4

C05

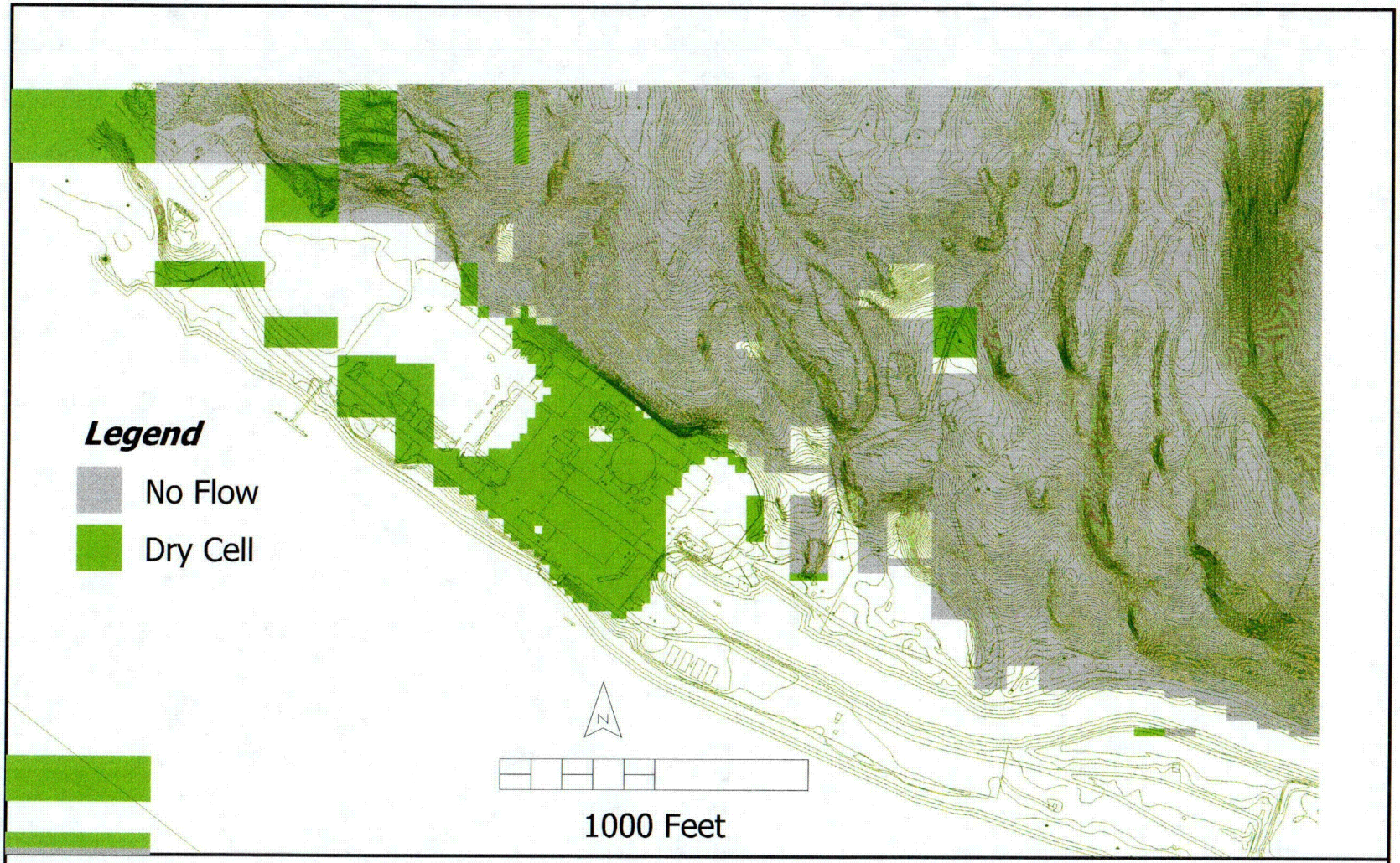

Figure 4A--Predicted Dry Cells, Plant Area

Shown for Top Layer of Model under Average Annual Recharge

Shown for Pre-Demolition Conditions

11/05/05

STRATEX
strategic consulting

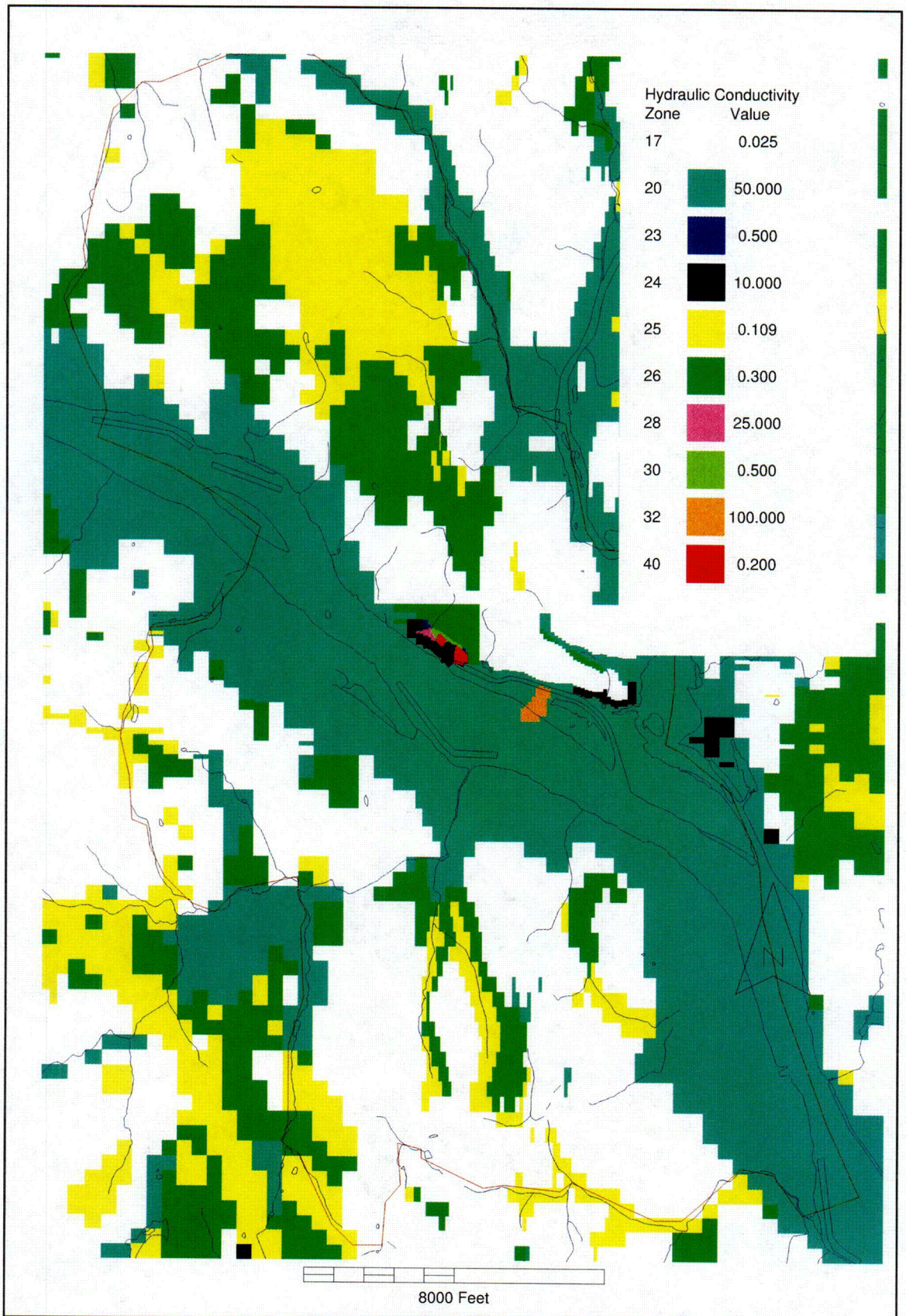

Figure 5--Hydraulic Conductivity for Layer 1

CY Groundwater Model

Values in legend are Kx values in feet/day

Refer to Table 1 for complete value description 8/22/05

STRATEX
strategic consulting

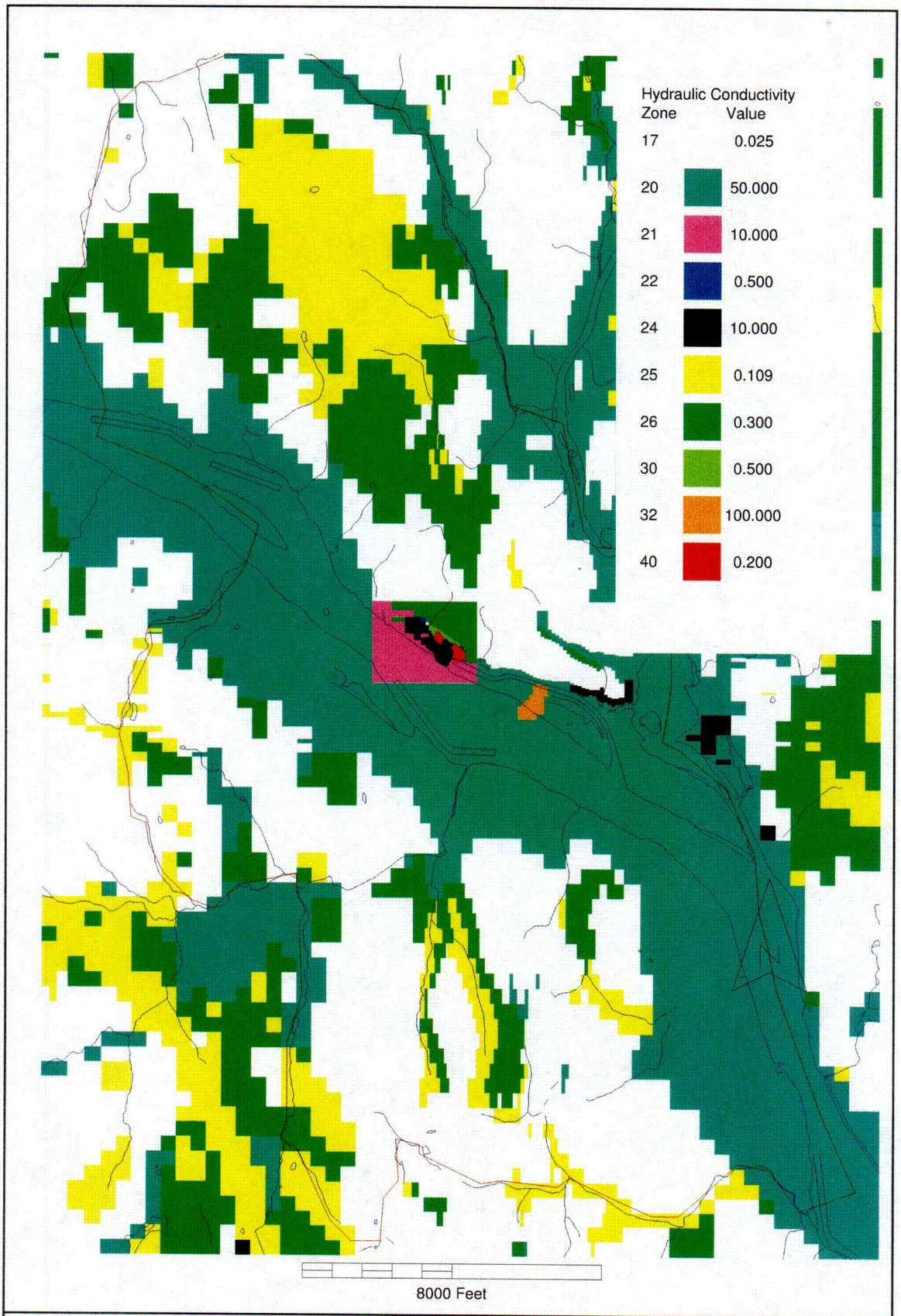

Figure 6--Hydraulic Conductivity for Layer 2

CY Groundwater Model

Values in legend are Kx values in feet/day

Refer to Table 1 for complete value description 8/22/05

STRATEX
strategic consulting

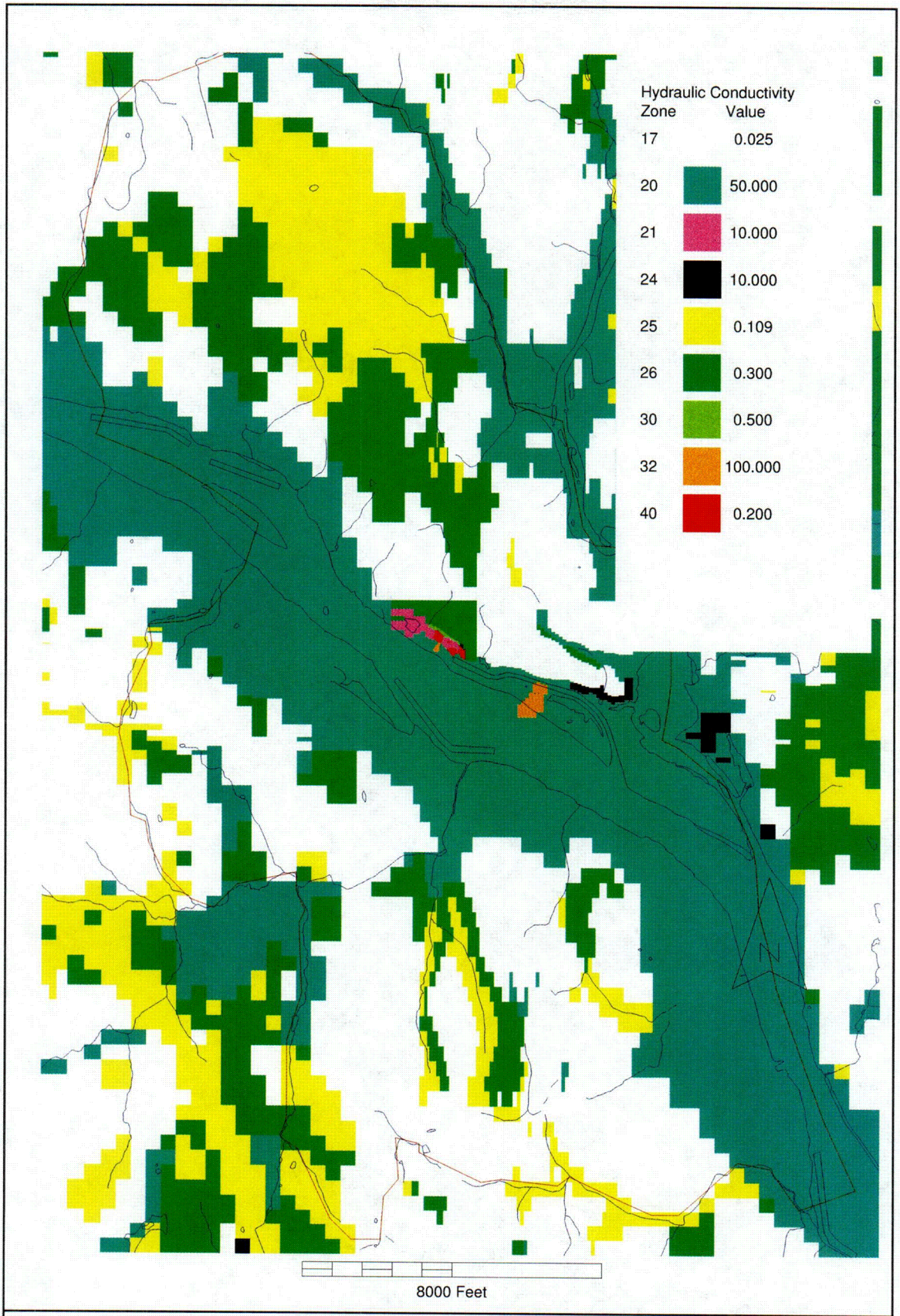

Figure 7--Hydraulic Conductivity for Layer 3

CY Groundwater Model

Values in legend are Kx values in feet/day

Refer to Table 1 for complete value description 8/22/05

STRATEX
strategic consulting

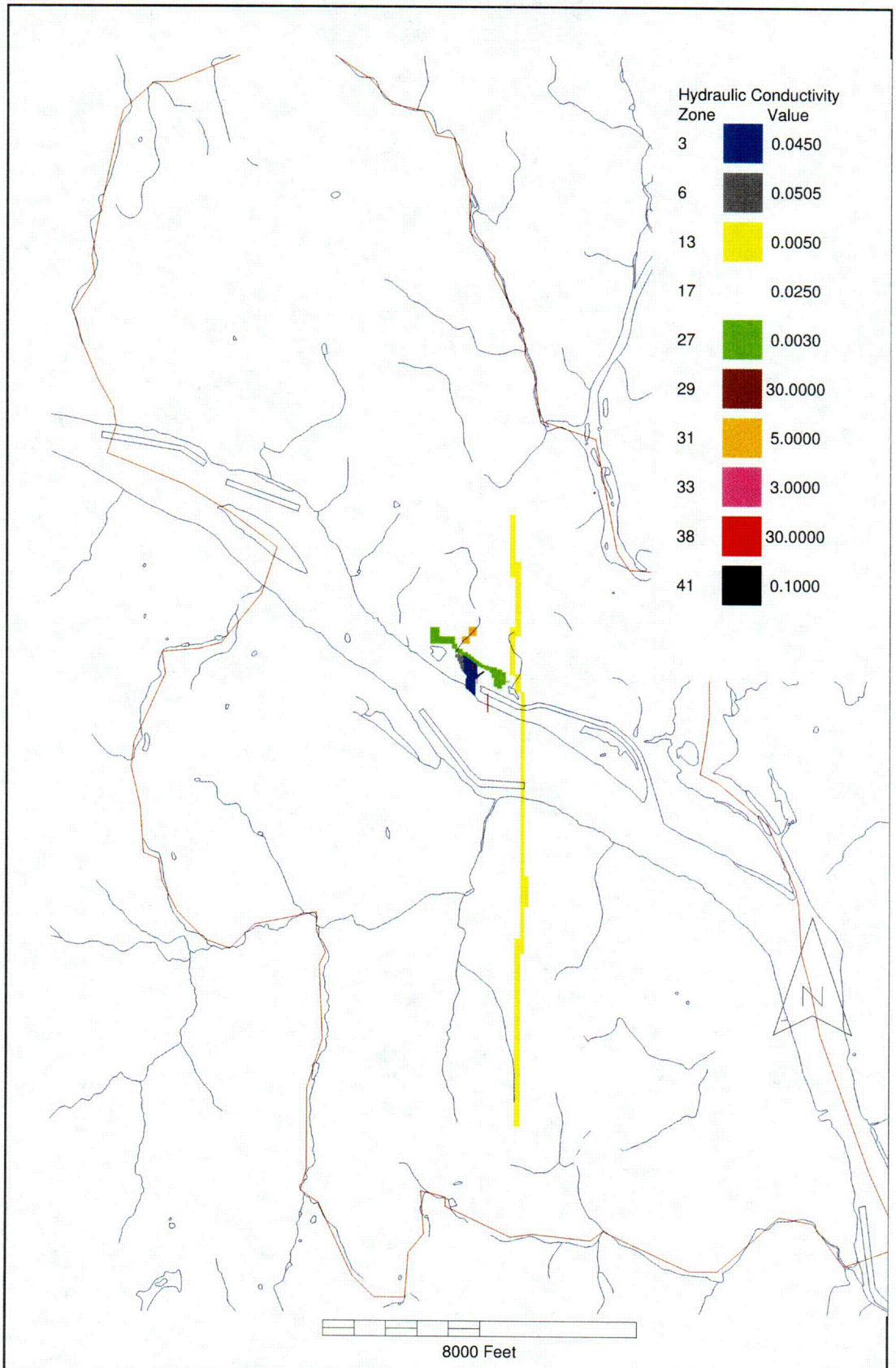

Figure 8--Hydraulic Conductivity for Layer 4

CY Groundwater Model

Values in legend are Kx values in feet/day

Refer to Table 1 for complete values 8/22/05

STRATEX
strategic consulting

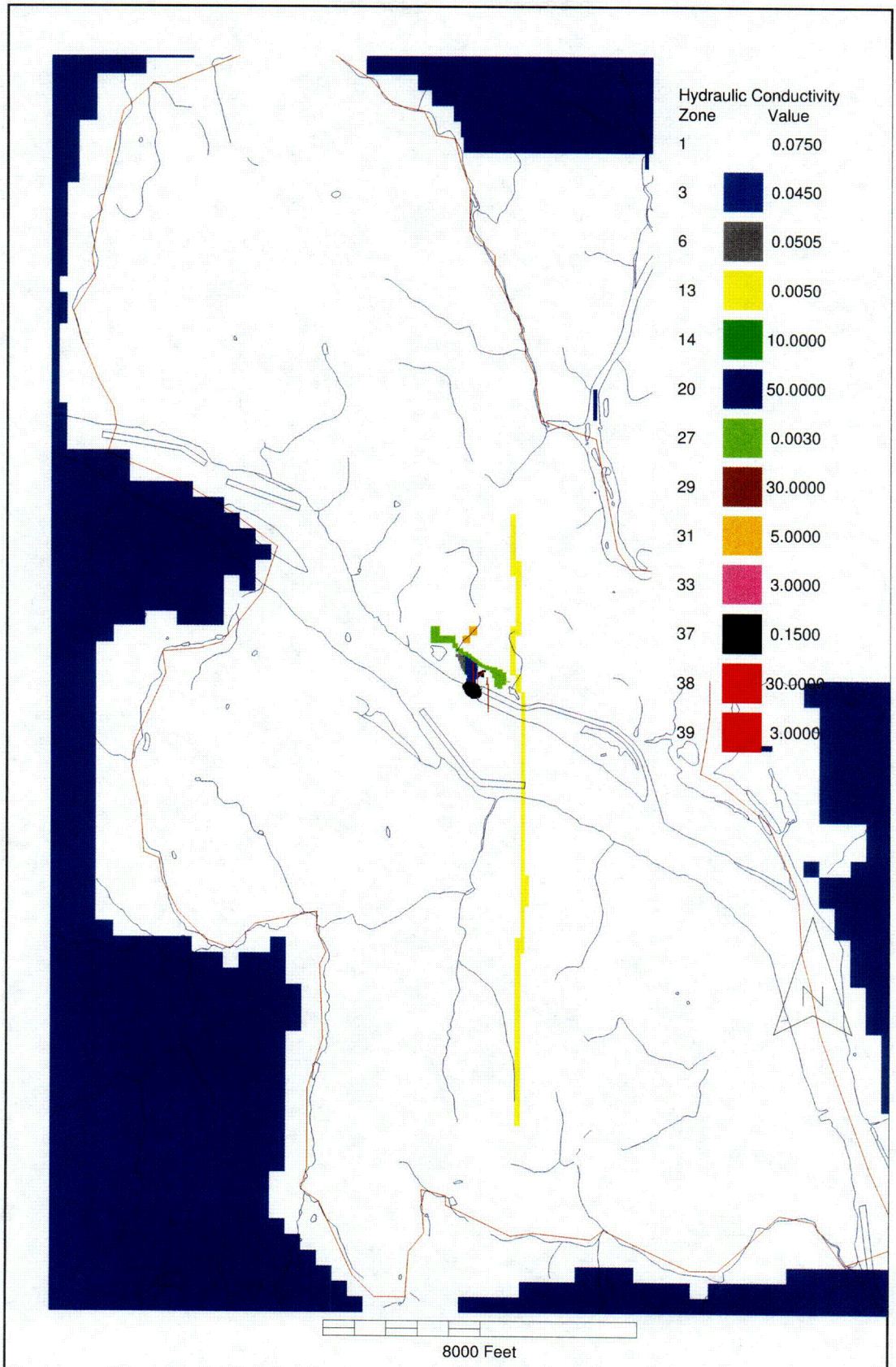

Figure 9--Hydraulic Conductivity for Layer 5

CY Groundwater Model

Values in legend are Kx values in feet/day

Refer to Table 1 for complete values 8/22/05

STRATEX
strategic consulting

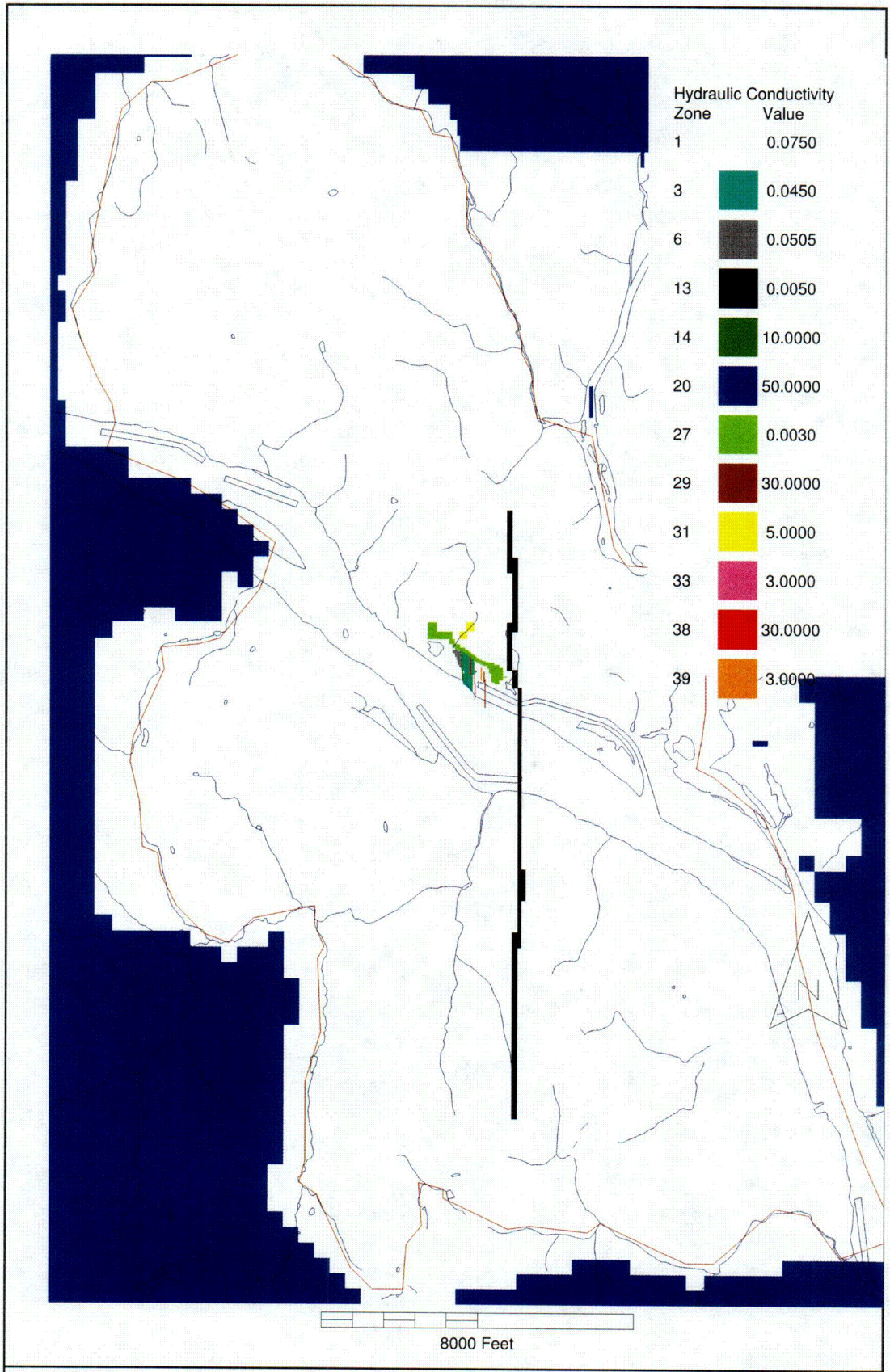

Figure 10--Hydraulic Conductivity for Layer 6

CY Groundwater Model

Values in legend are Kx values in feet/day

Refer to Table 1 for complete values 8/22/05

STRATEX
strategic consulting

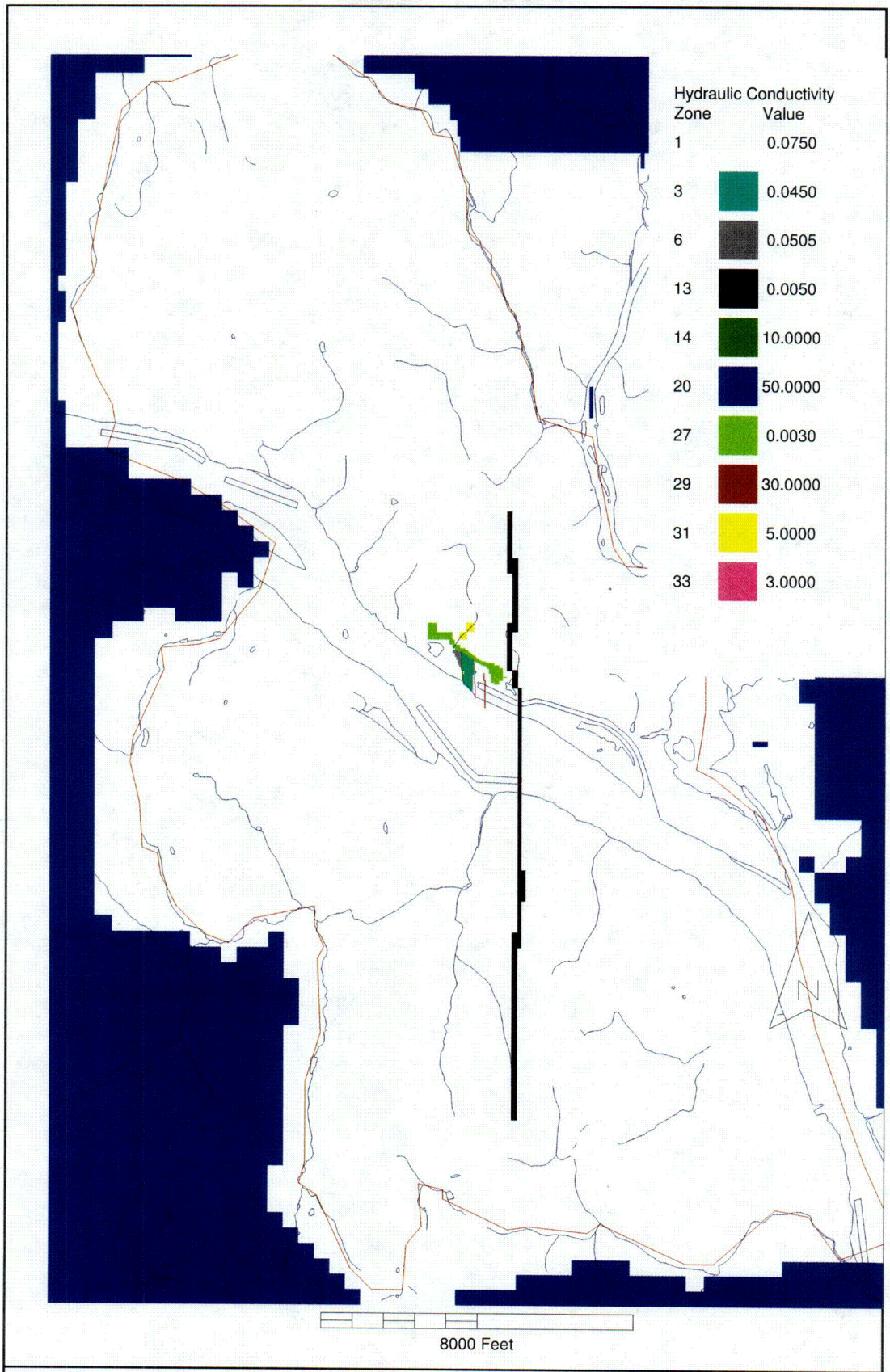

Figure 11--Hydraulic Conductivity for Layer 7

CY Groundwater Model

Values in legend are Kx values in feet/day

Refer to Table 1 for complete values 8/22/05

STRATEX
strategic consulting

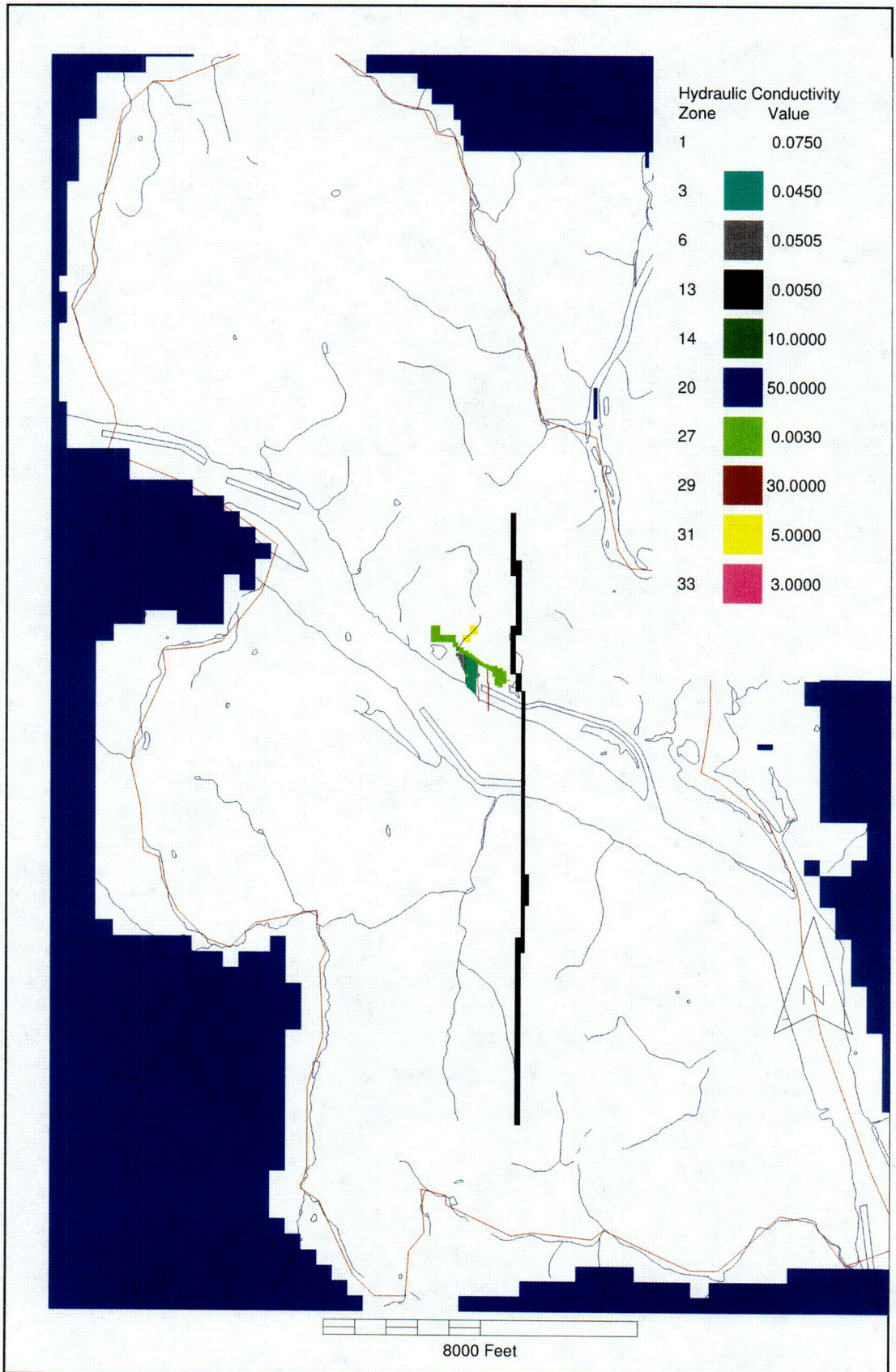

Figure 12--Hydraulic Conductivity for Layer 8

CY Groundwater Model

Values in legend are Kx values in feet/day

Refer to Table 1 for complete values 8/22/05

STRATEX
strategic consulting

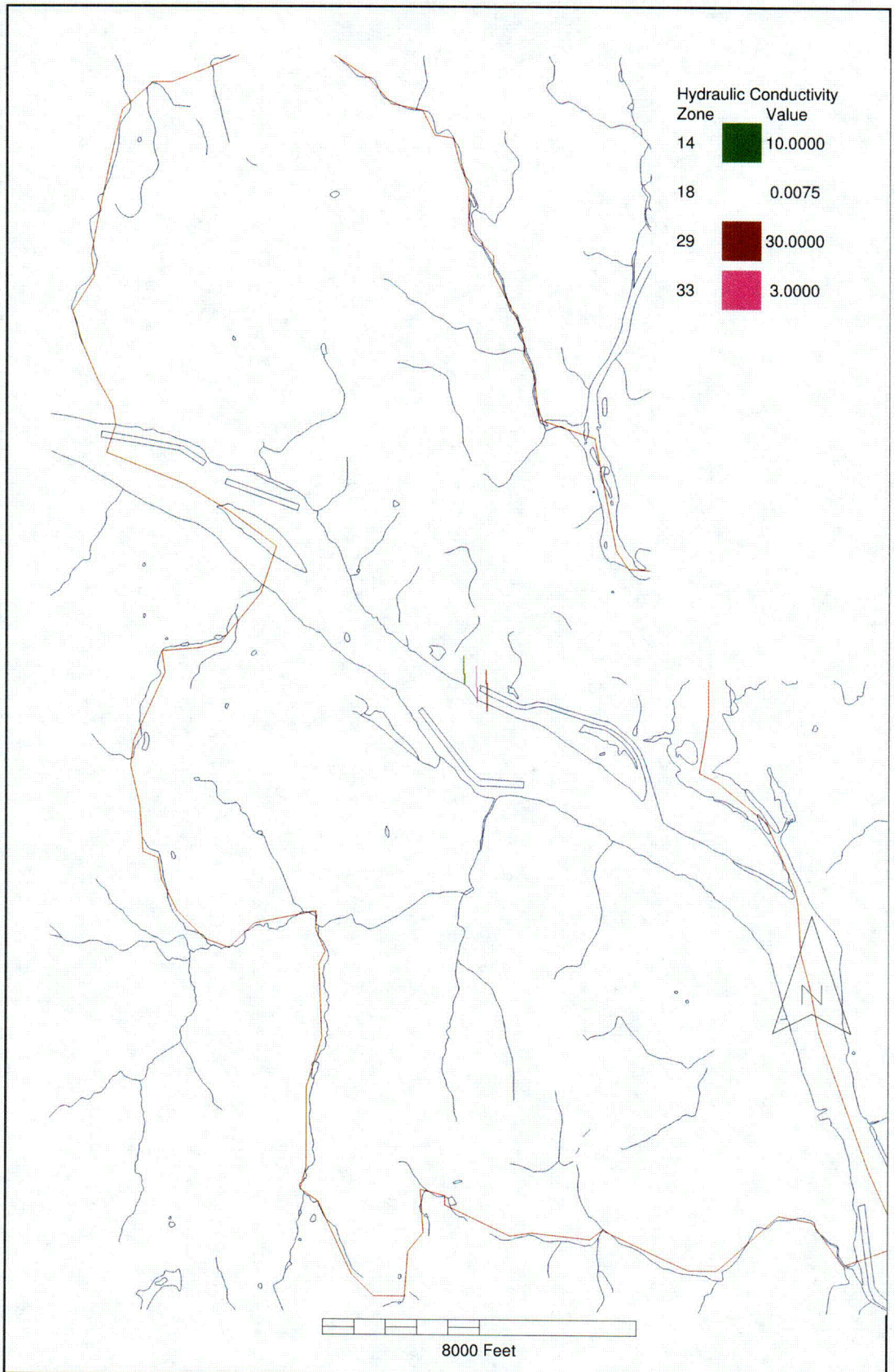

Figure 13--Hydraulic Conductivity for Layer 9

CY Groundwater Model

Values in legend are Kx values in feet/day

Refer to Table 1 for complete values 8/22/05

STRATEX
strategic consulting

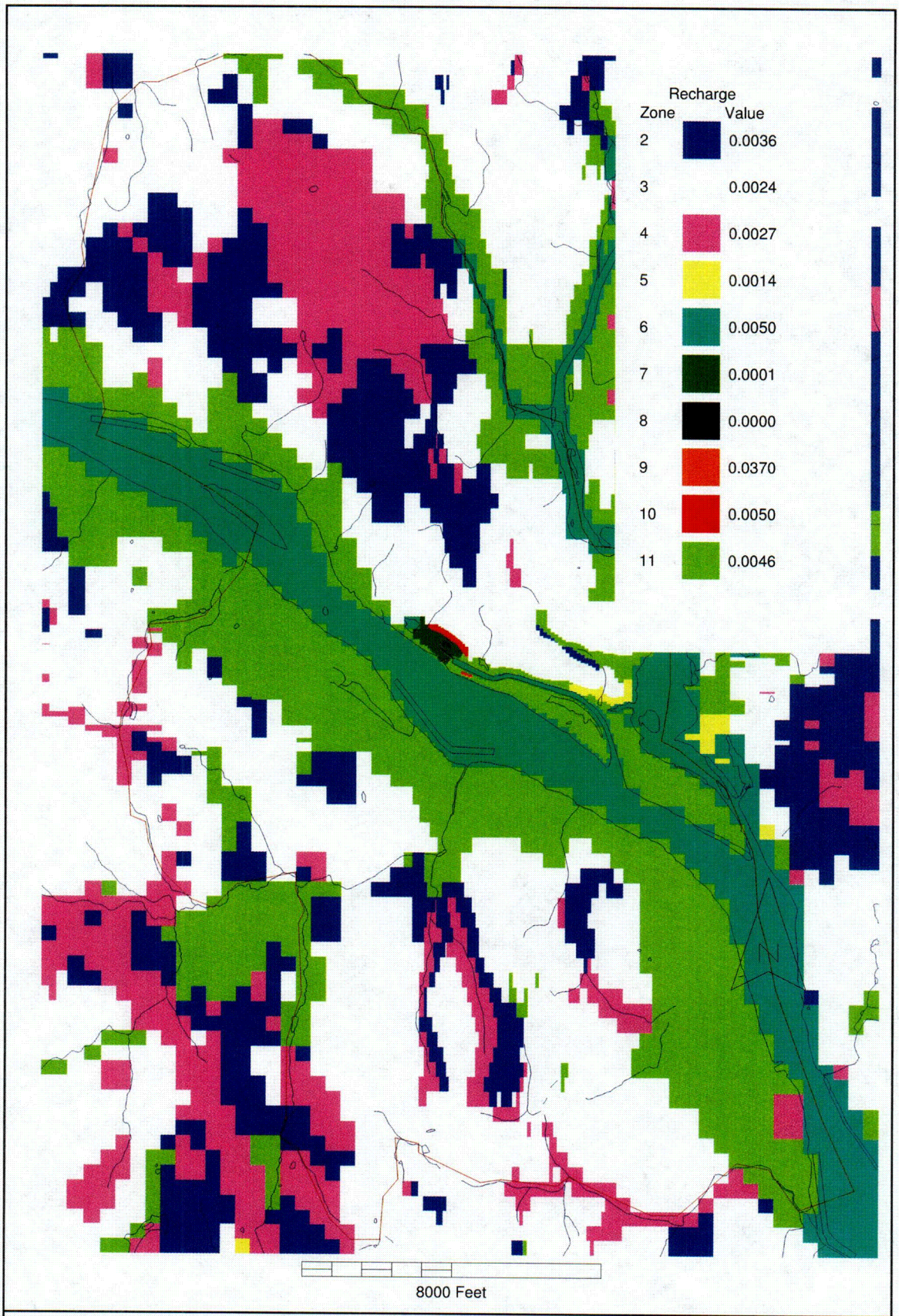

Figure 14--Ave. Annual Precip. Recharge Rates

CY Groundwater Model

Values in legend are rates in feet/day

Refer to Table 2 for complete value description 8/22/05

STRATEX
strategic consulting

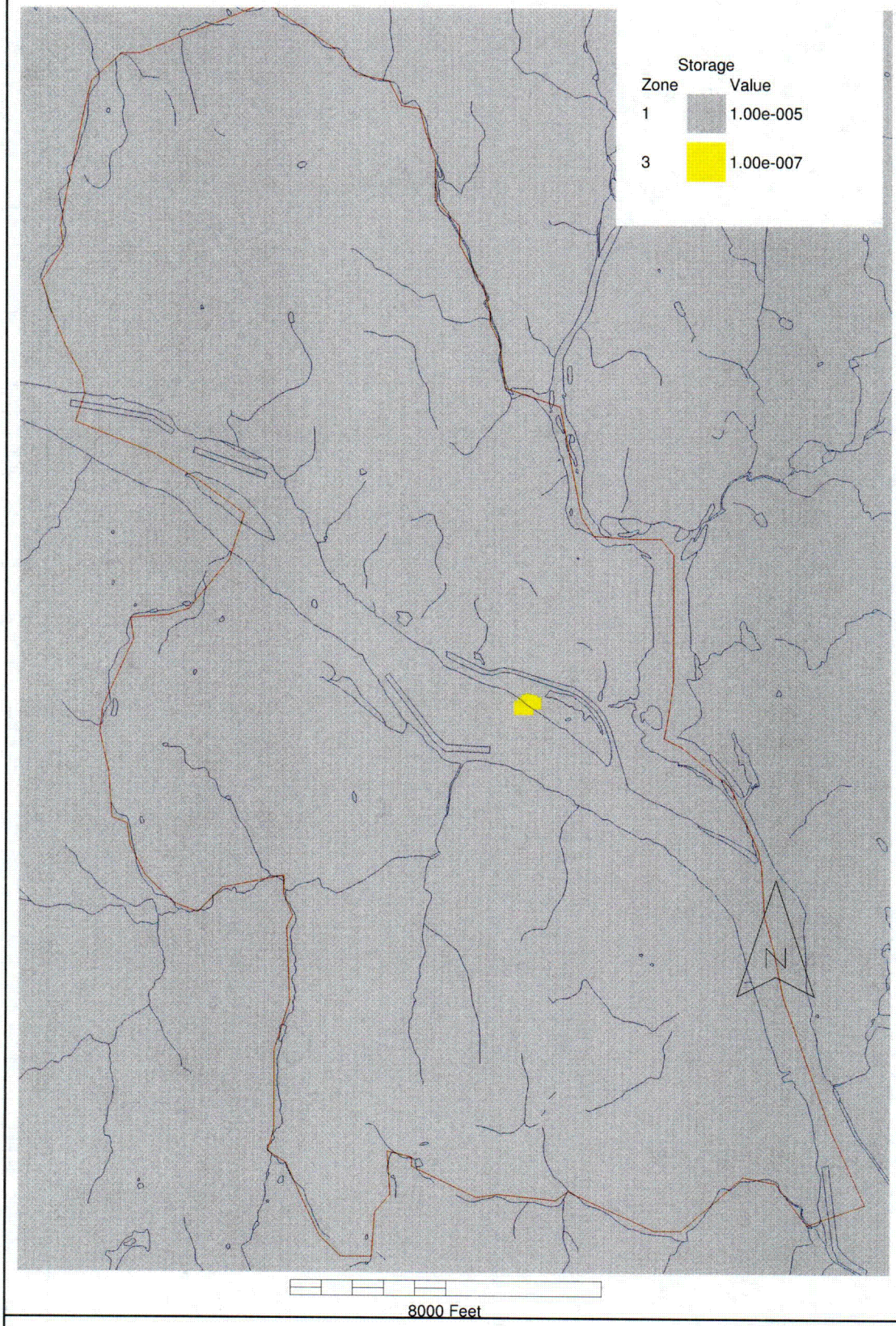

Figure 15--Specific Storage for Layer 2

CY Groundwater Model

Values in legend are rates in 1/feet

Refer to Table 3 for complete value description including specific yield and porosity 8/22/05

STRATEX
strategic consulting

Figure 16--May 2004 Tide Effects on Monitoring Wells
CY Groundwater Model

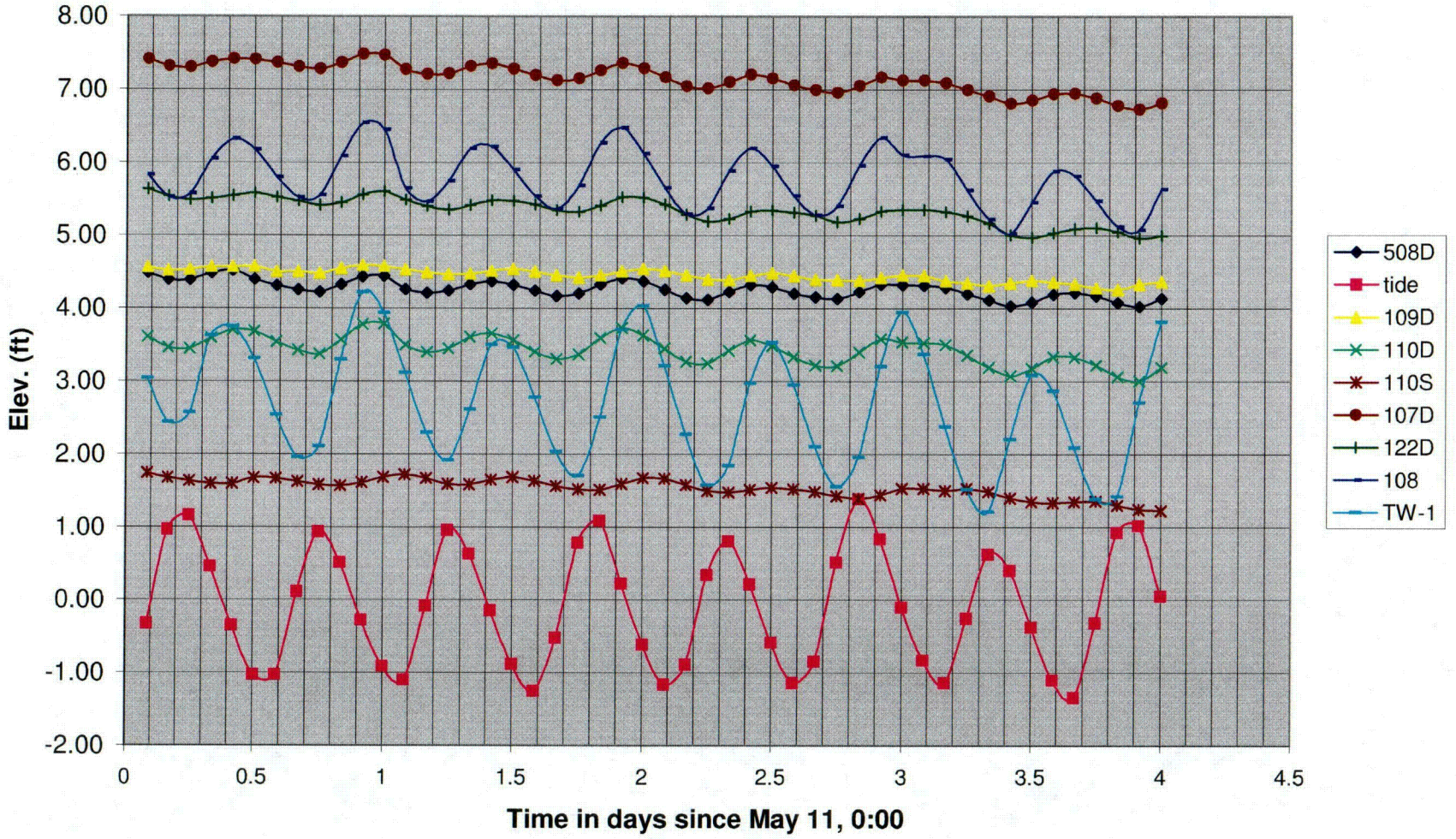

C18

Figure 17
Cumulative Precipitation at Haddam 2004
CY Groundwater Model

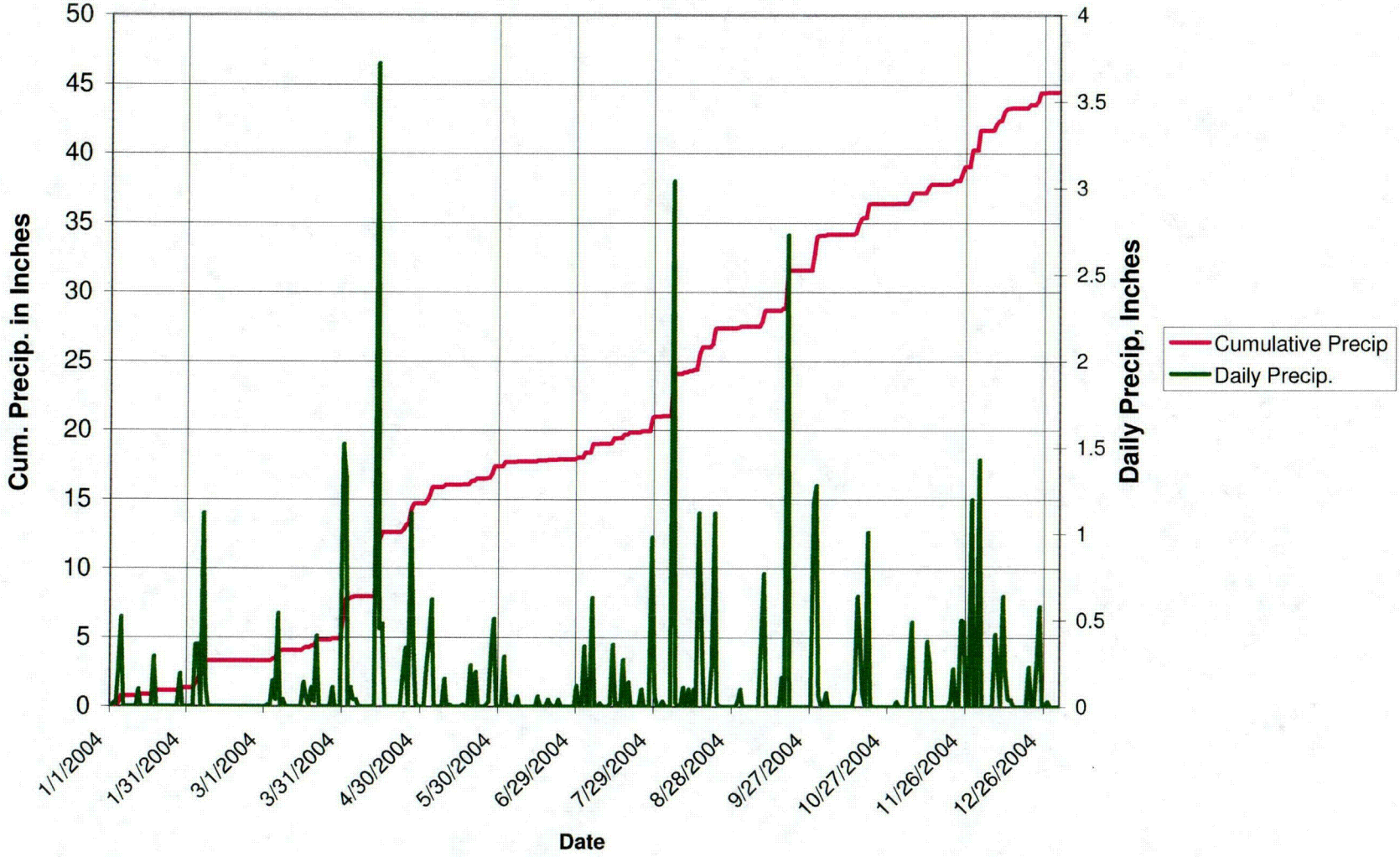

Figure 18

Steady-State Calibration, Observed Heads vs. Computed Heads, CY Groundwater Model

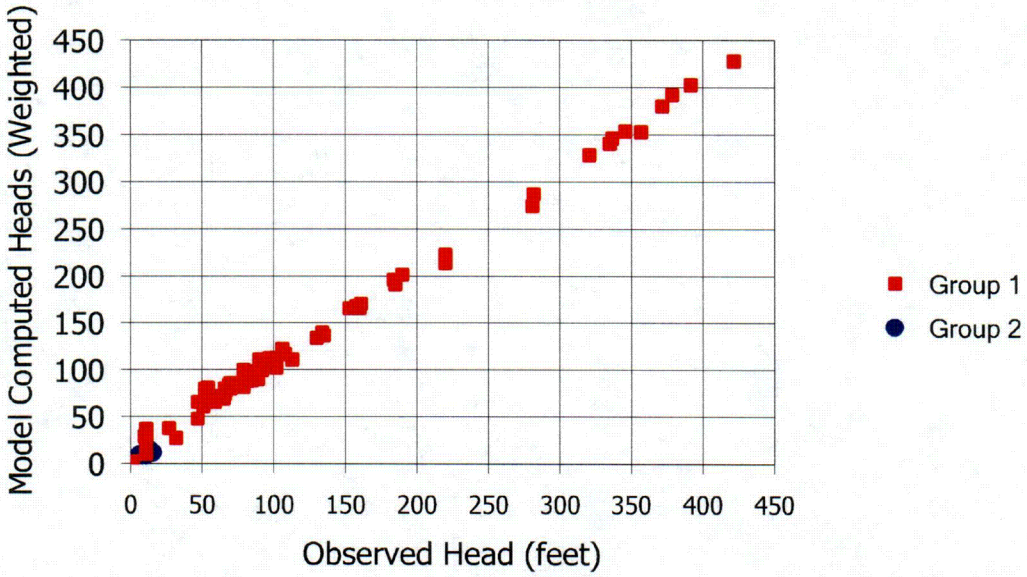

Figure 19

Steady-State Calibration, Observed Heads vs. Residuals, CY Groundwater Model

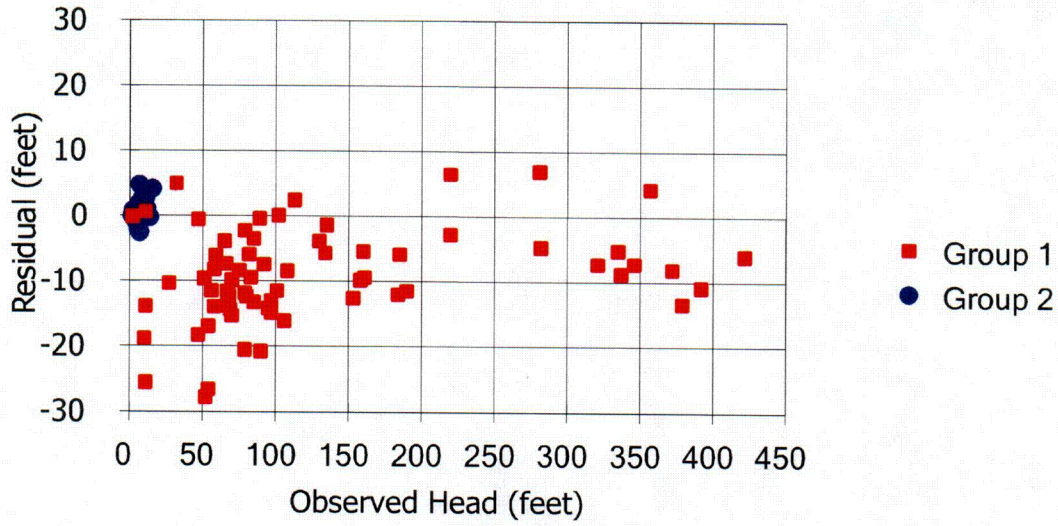

Figure 20

Observed vs. Computed Target Values, May 2004 Tidal Response Simulation CY Groundwater Model

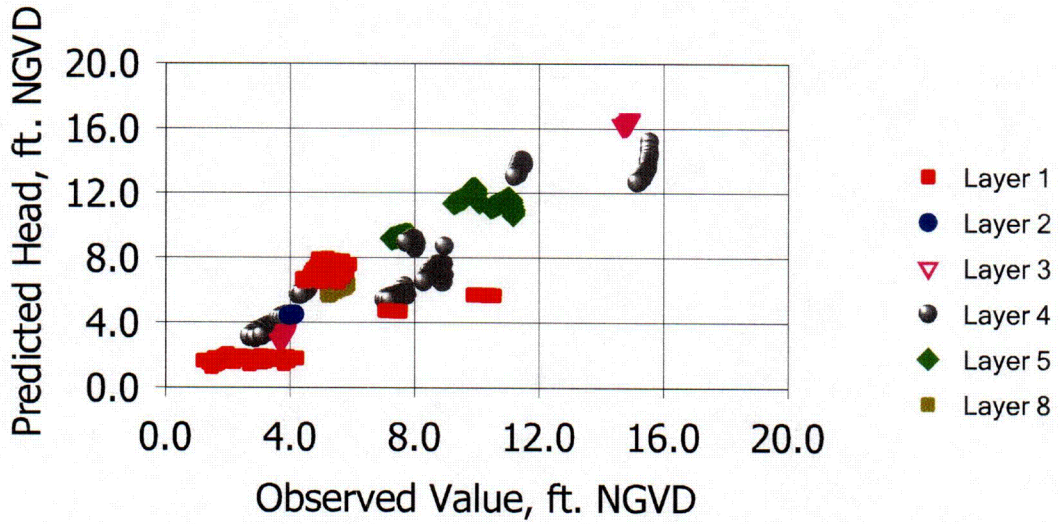

Figure 21

Observed vs. Computed Target Values, September 2004 Pumping Test Simulation CY Groundwater Model

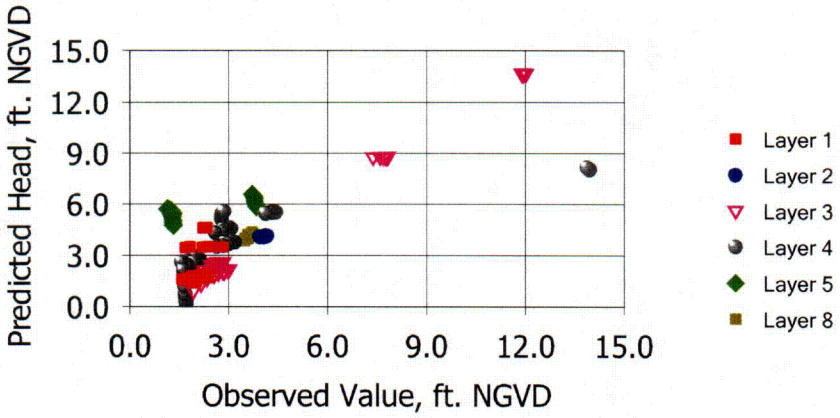

Figure 22

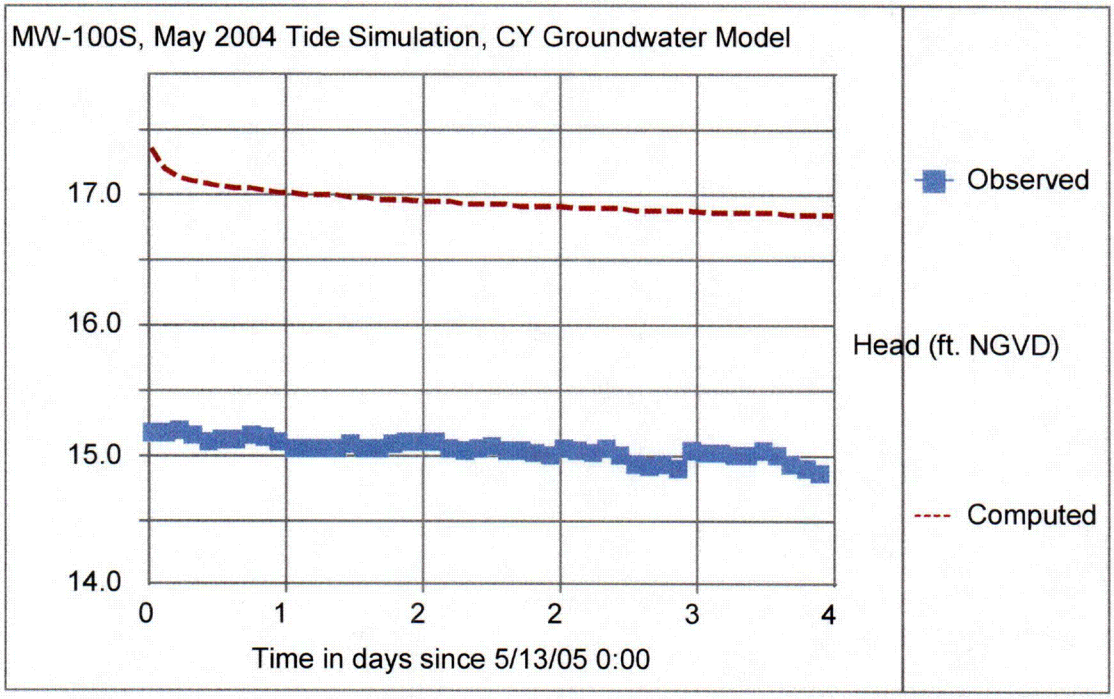
MW-100S, May 2004 Tide Simulation, CY Groundwater Model
17.0
16.0
15.0
14.0
0
1
2
2
3
4
Time in days since 5/13/05 0:00
Head (ft. NGVD)
Observed
Computed

(a)

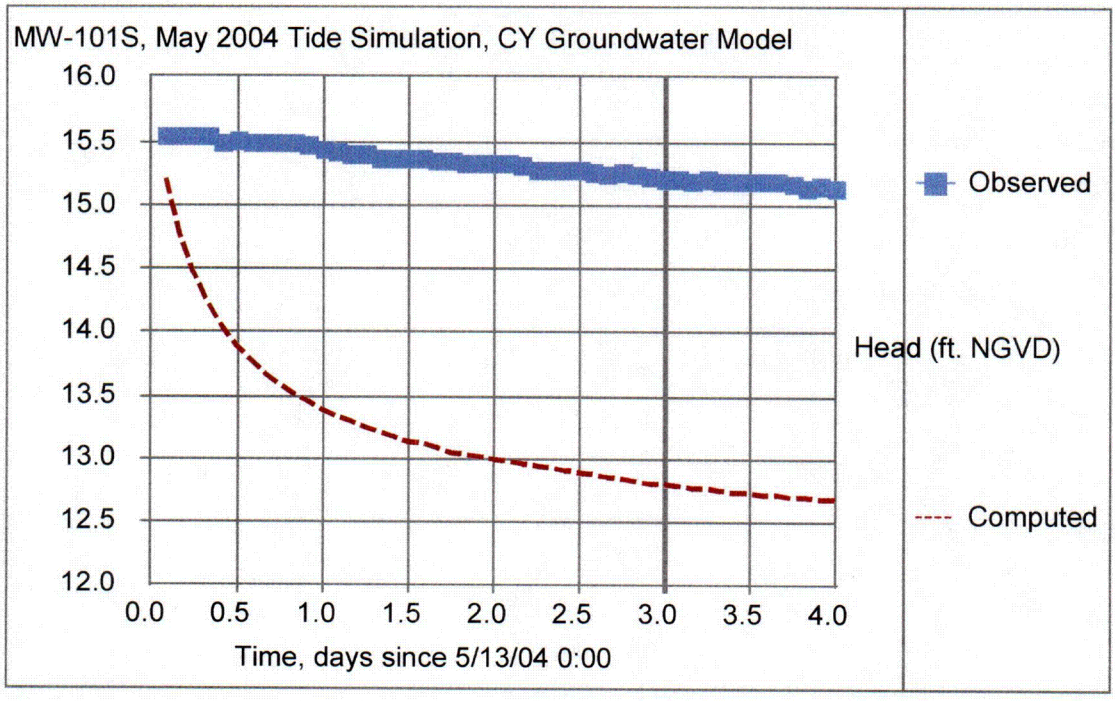
MW-101S, May 2004 Tide Simulation, CY Groundwater Model
16.0
15.5
15.0
14.5
14.0
13.5
13.0
12.5
12.0
0.0
0.5
1.0
1.5
2.0
2.5
3.0
3.5
4.0
Time, days since 5/13/04 0:00
Head (ft. NGVD)
Observed
Computed

(b)

Figure 22

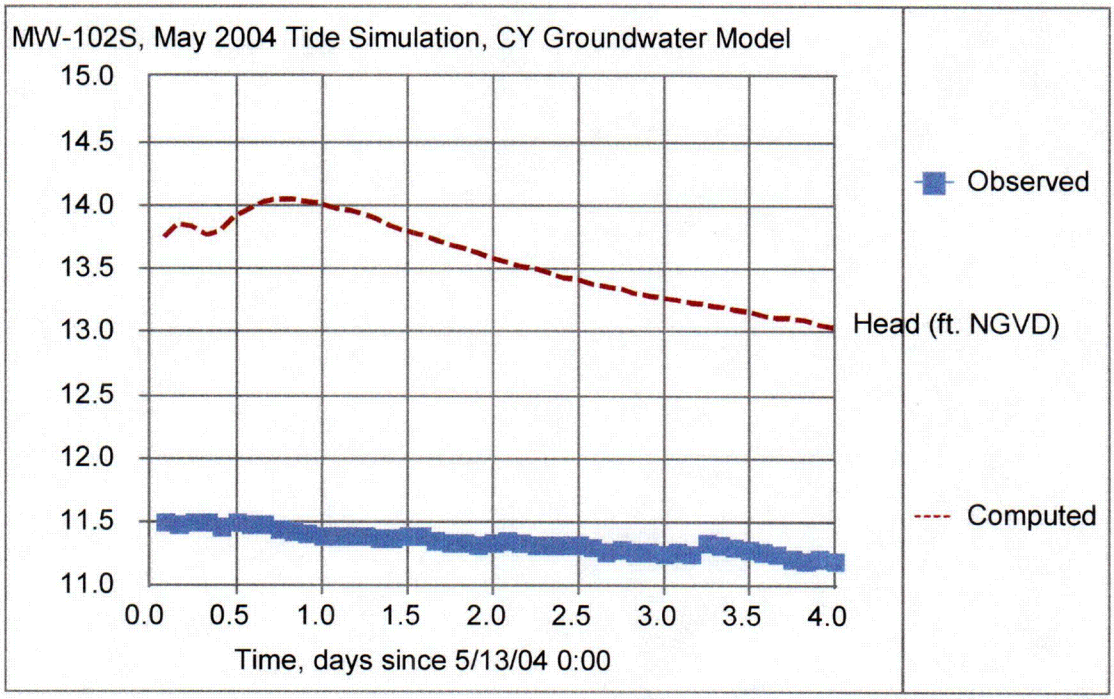
MW-102S, May 2004 Tide Simulation, CY Groundwater Model
15.0
14.5
14.0
13.5
13.0
12.5
12.0
11.5
11.0
0.0
0.5
1.0
1.5
2.0
2.5
3.0
3.5
4.0
Time, days since 5/13/04 0:00
Head (ft. NGVD)
Observed
Computed

(c)

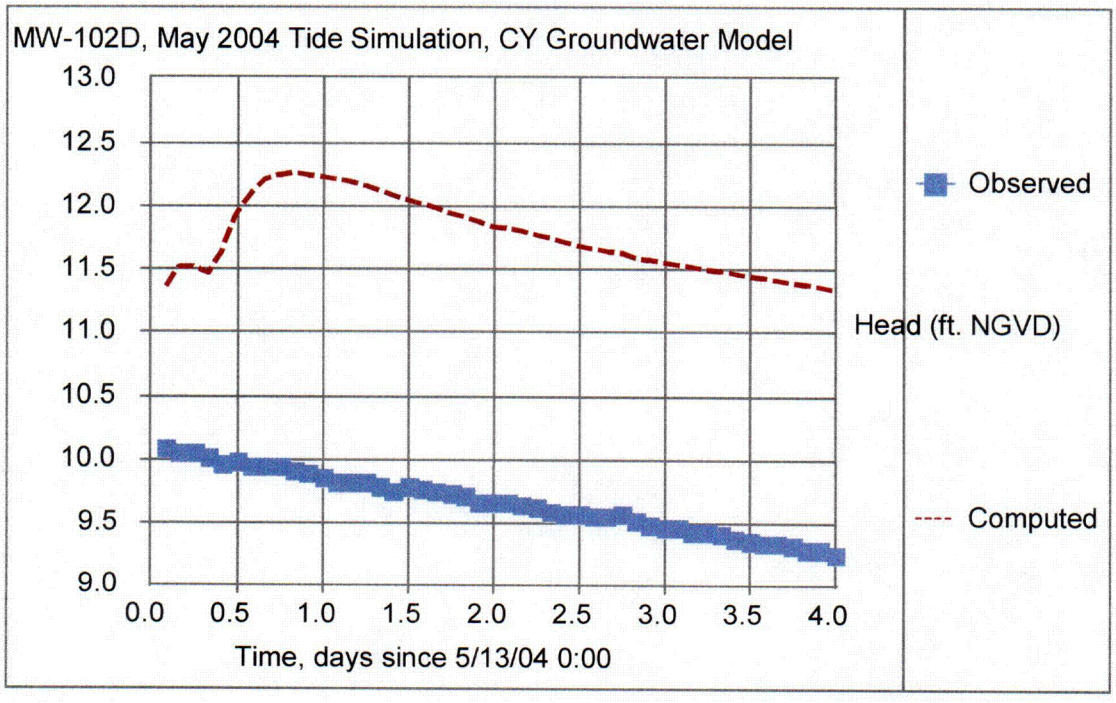
MW-102D, May 2004 Tide Simulation, CY Groundwater Model
13.0
12.5
12.0
11.5
11.0
10.5
10.0
9.5
9.0
0.0
0.5
1.0
1.5
2.0
2.5
3.0
3.5
4.0
Time, days since 5/13/04 0:00
Head (ft. NGVD)
Observed
Computed

(d)

Figure 22

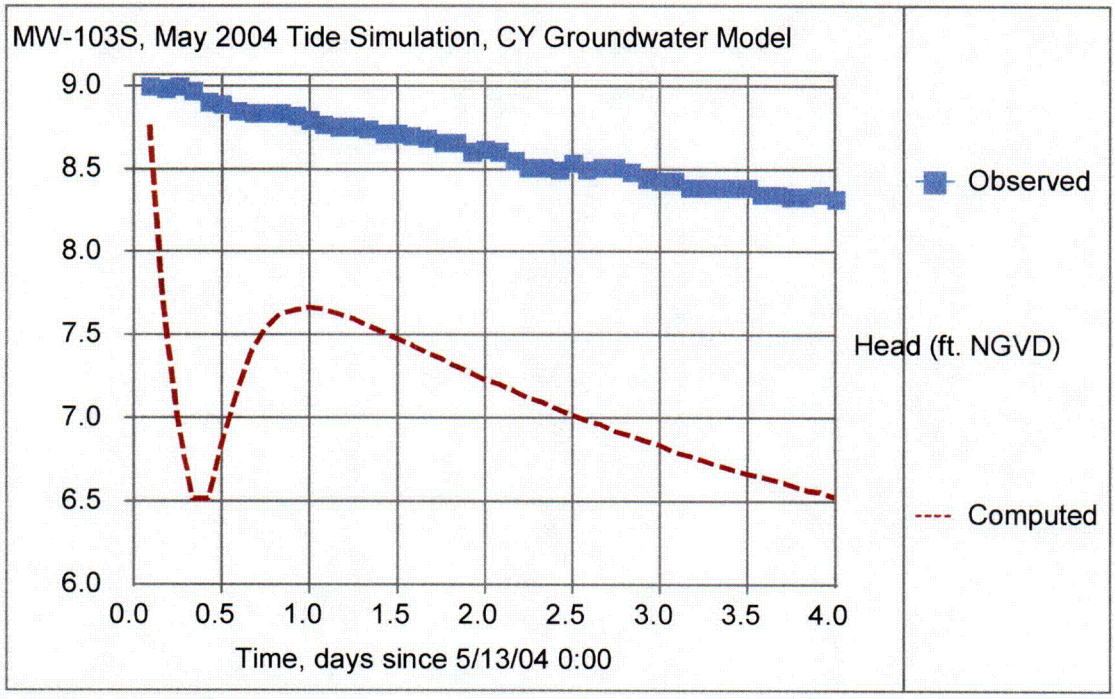
MW-103S, May 2004 Tide Simulation, CY Groundwater Model
9.0
8.5
8.0
7.5
7.0
6.5
6.0
0.0
0.5
1.0
1.5
2.0
2.5
3.0
3.5
4.0
Time, days since 5/13/04 0:00
Head (ft. NGVD)
Observed
Computed

(e)

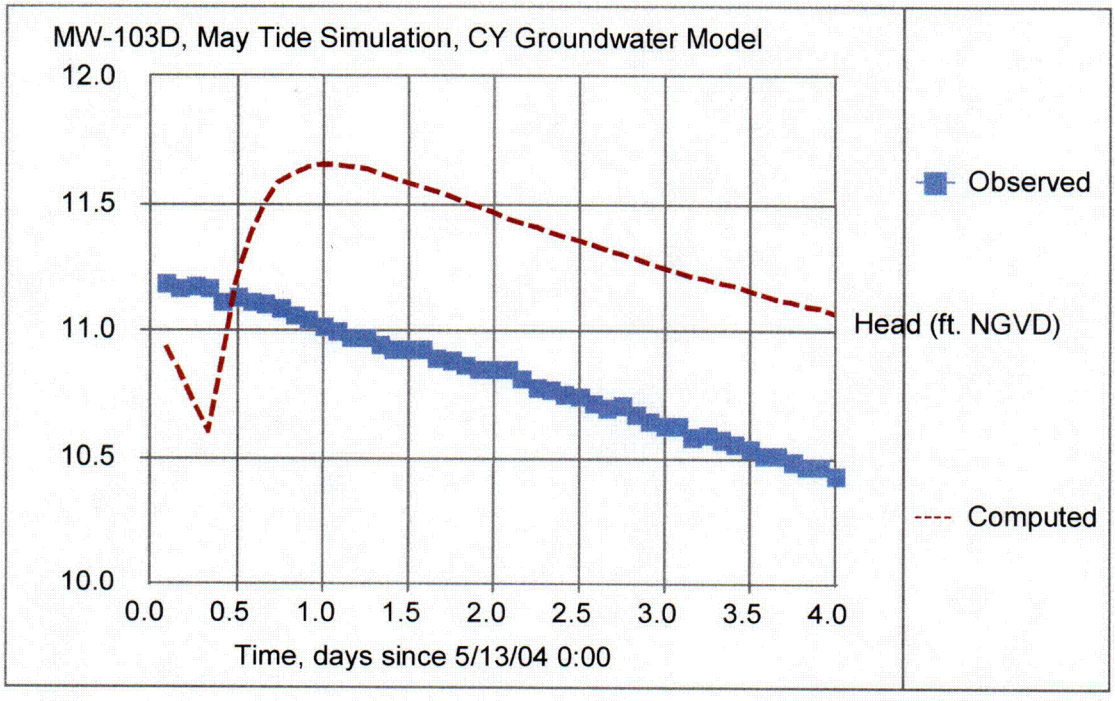
MW-103D, May Tide Simulation, CY Groundwater Model
12.0
11.5
11.0
10.5
10.0
0.0
0.5
1.0
1.5
2.0
2.5
3.0
3.5
4.0
Time, days since 5/13/04 0:00
Head (ft. NGVD)
Observed
Computed

(f)

Figure 22

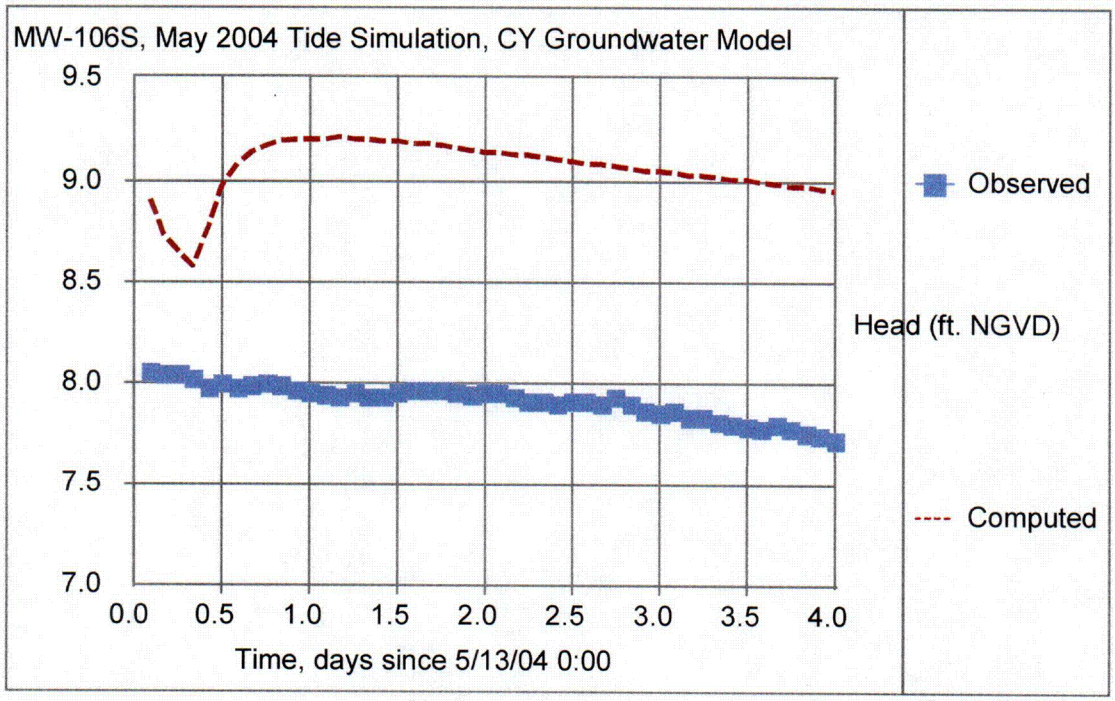
MW-106S, May 2004 Tide Simulation, CY Groundwater Model
9.5
9.0
8.5
8.0
7.5
7.0
0.0
0.5
1.0
1.5
2.0
2.5
3.0
3.5
4.0
Time, days since 5/13/04 0:00
Head (ft. NGVD)
Observed
Computed

(g)

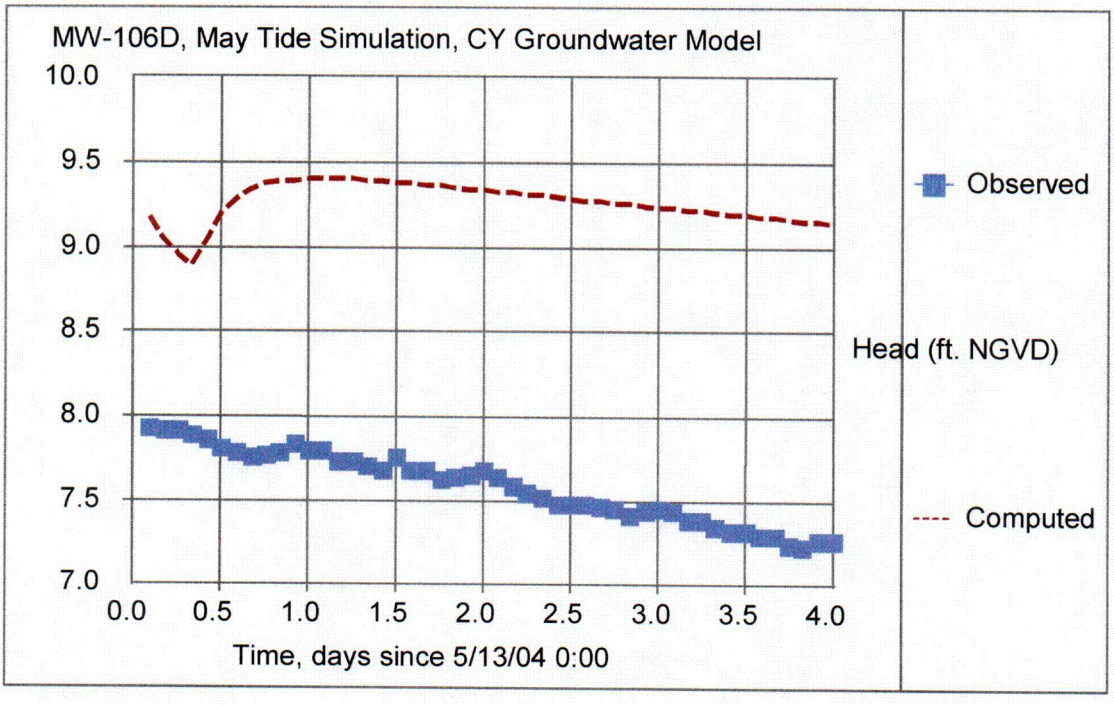
MW-106D, May Tide Simulation, CY Groundwater Model
10.0
9.5
9.0
8.5
8.0
7.5
7.0
0.0
0.5
1.0
1.5
2.0
2.5
3.0
3.5
4.0
Time, days since 5/13/04 0:00
Head (ft. NGVD)
Observed
Computed

(h)

Figure 22

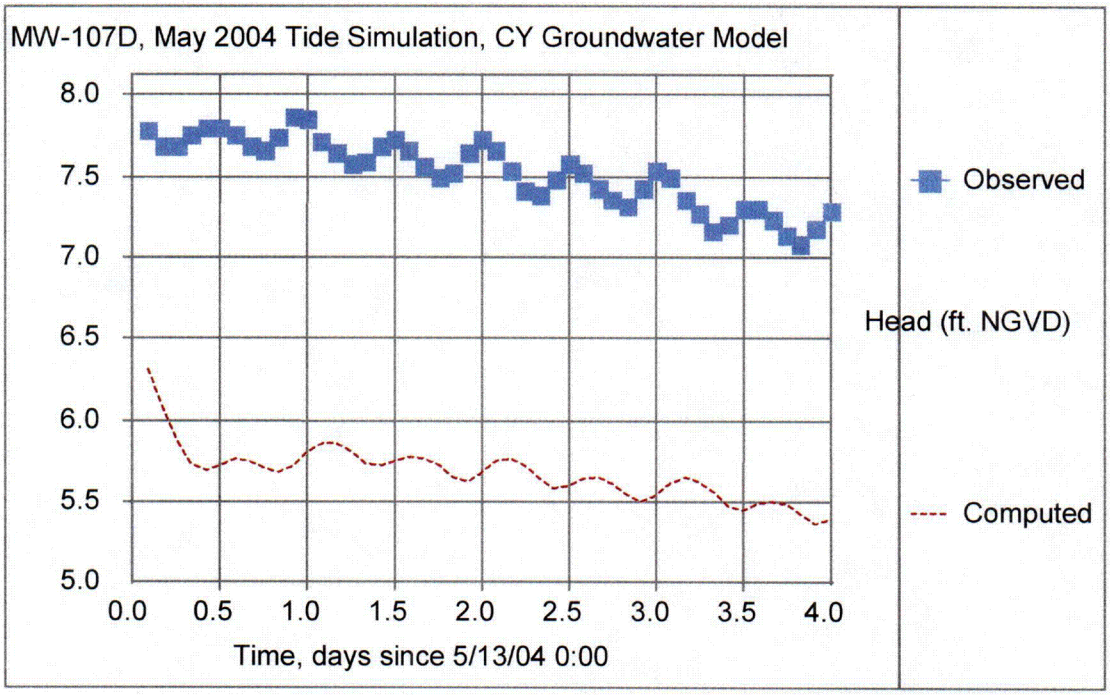
MW-107D, May 2004 Tide Simulation, CY Groundwater Model
8.0
7.5
7.0
6.5
6.0
5.5
5.0
0.0
0.5
1.0
1.5
2.0
2.5
3.0
3.5
4.0
Time, days since 5/13/04 0:00
Observed
Head (ft. NGVD)
Computed

(i)

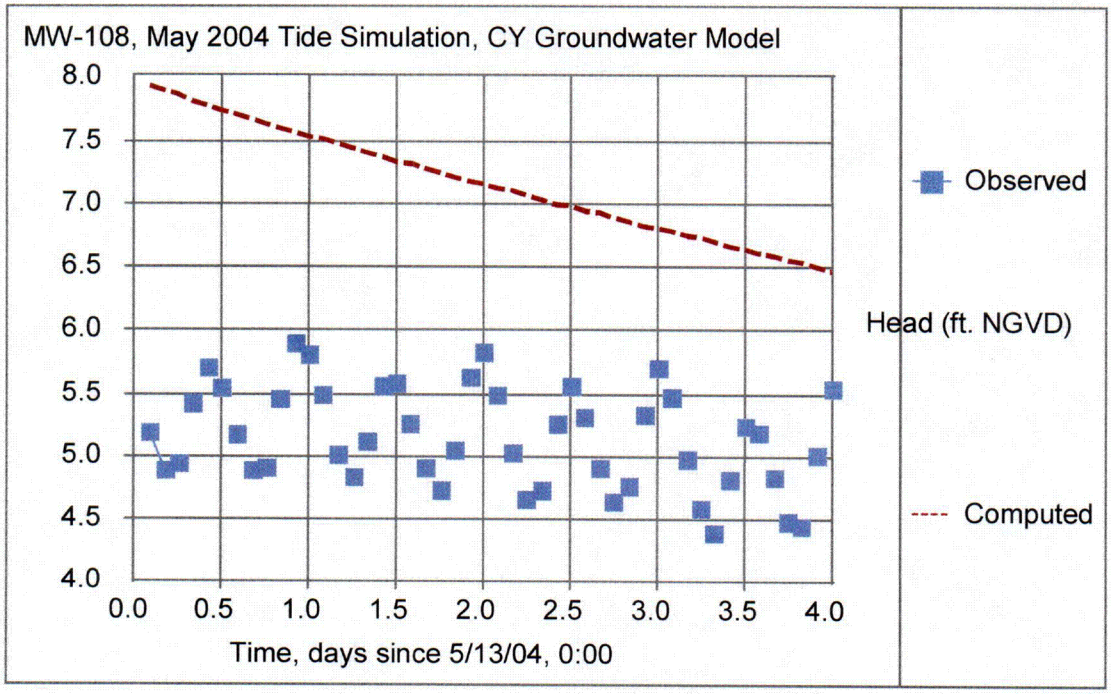
MW-108, May 2004 Tide Simulation, CY Groundwater Model
8.0
7.5
7.0
6.5
6.0
5.5
5.0
4.5
4.0
0.0
0.5
1.0
1.5
2.0
2.5
3.0
3.5
4.0
Time, days since 5/13/04, 0:00
Observed
Head (ft. NGVD)
Computed

(j)

Figure 22

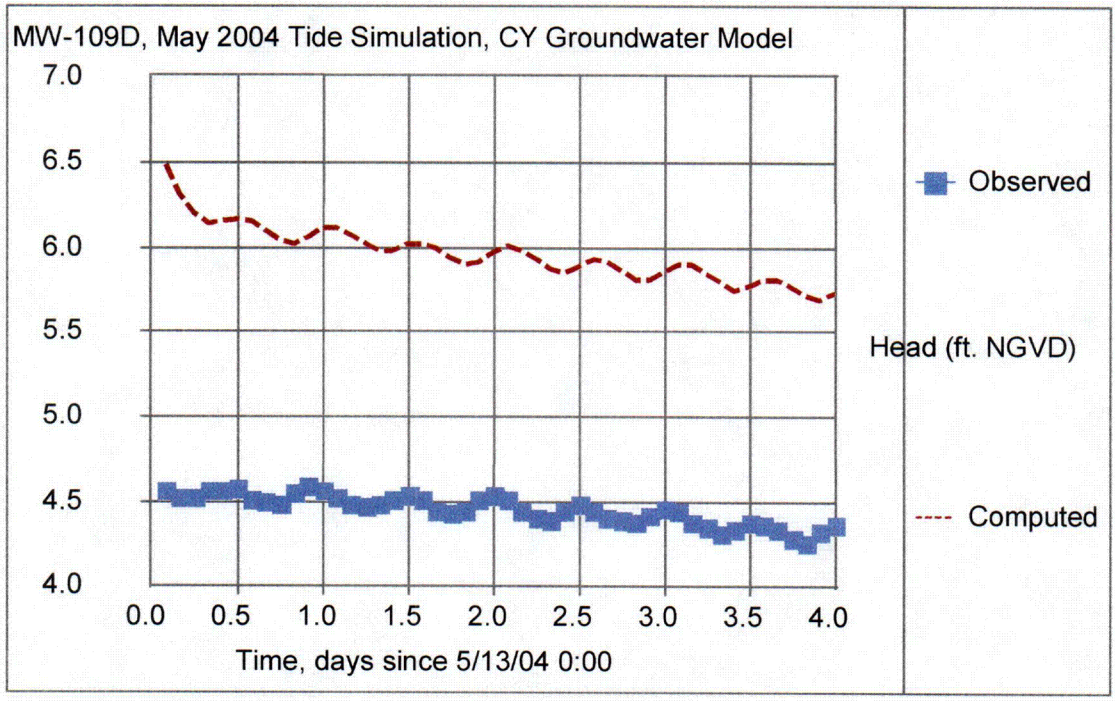
MW-109D, May 2004 Tide Simulation, CY Groundwater Model
7.0
6.5
6.0
5.5
5.0
4.5
4.0
0.0
0.5
1.0
1.5
2.0
2.5
3.0
3.5
4.0
Time, days since 5/13/04 0:00
Head (ft. NGVD)
Observed
Computed

(k)

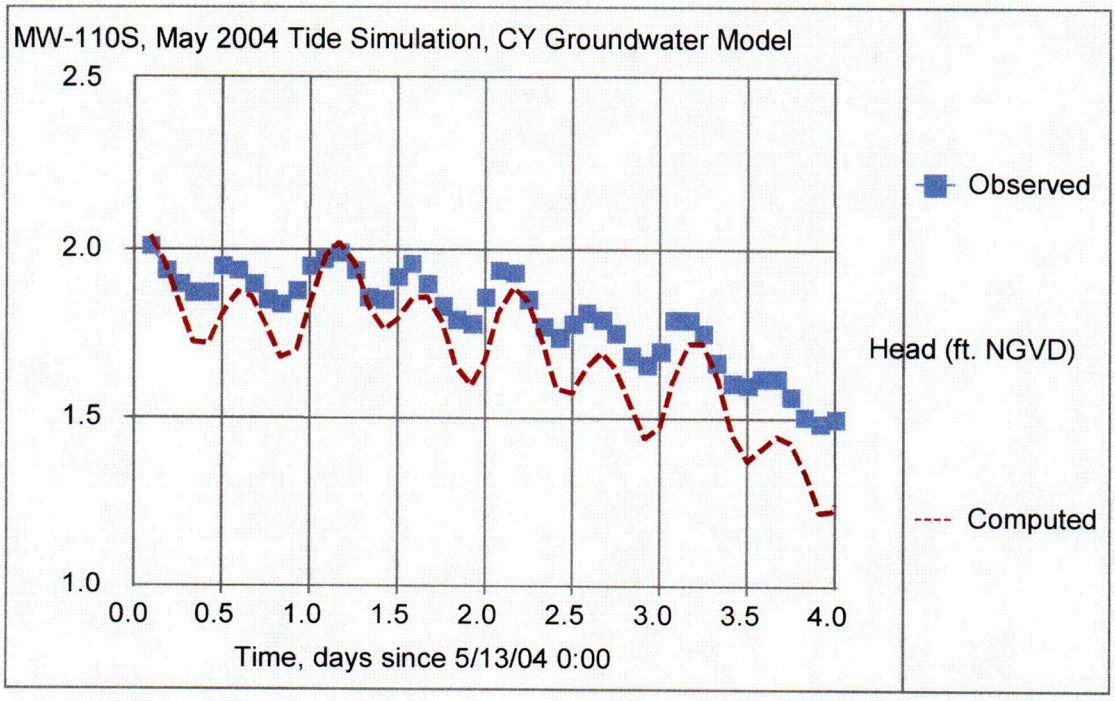
MW-110S, May 2004 Tide Simulation, CY Groundwater Model
2.5
2.0
1.5
1.0
0.0
0.5
1.0
1.5
2.0
2.5
3.0
3.5
4.0
Time, days since 5/13/04 0:00
Head (ft. NGVD)
Observed
Computed

(l)

Figure 22

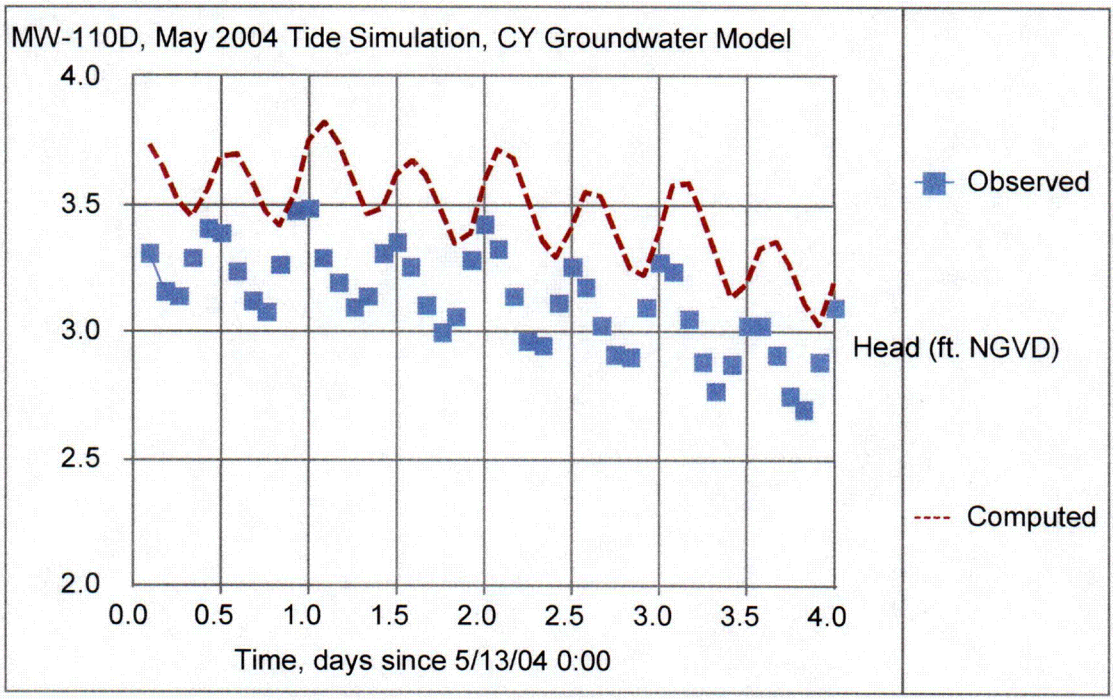
MW-110D, May 2004 Tide Simulation, CY Groundwater Model
4.0
3.5
3.0
2.5
2.0
0.0
0.5
1.0
1.5
2.0
2.5
3.0
3.5
4.0
Time, days since 5/13/04 0:00
Observed
Head (ft. NGVD)
Computed

(m)

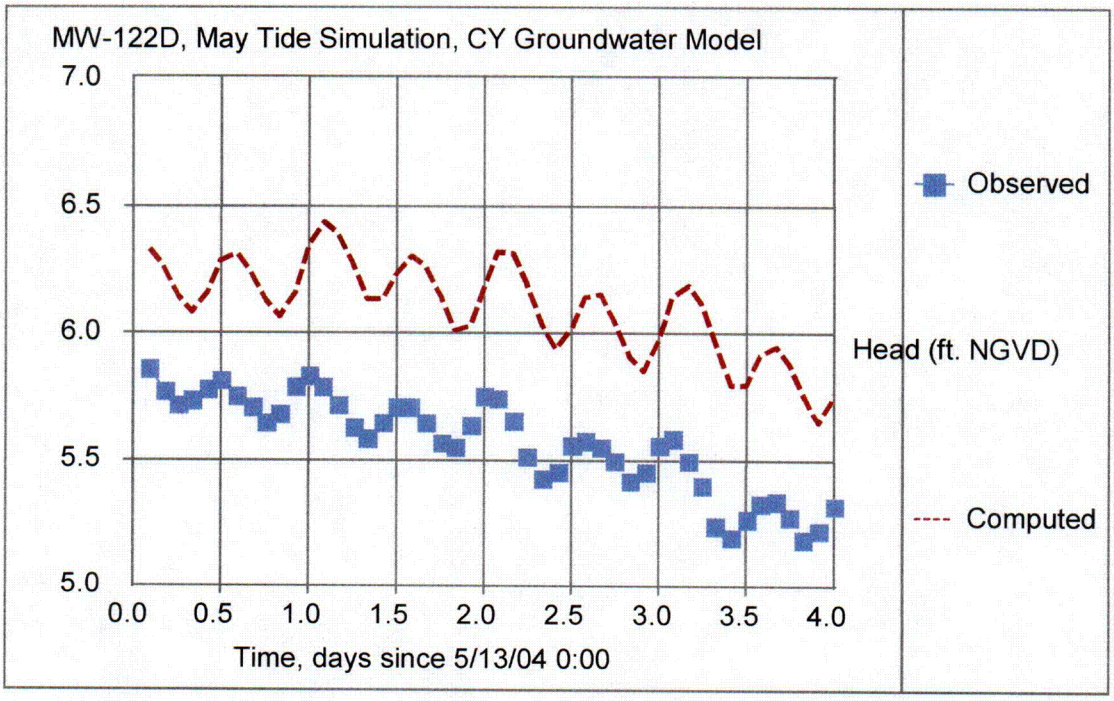
MW-122D, May Tide Simulation, CY Groundwater Model
7.0
6.5
6.0
5.5
5.0
0.0
0.5
1.0
1.5
2.0
2.5
3.0
3.5
4.0
Time, days since 5/13/04 0:00
Observed
Head (ft. NGVD)
Computed

(n)

Figure 22

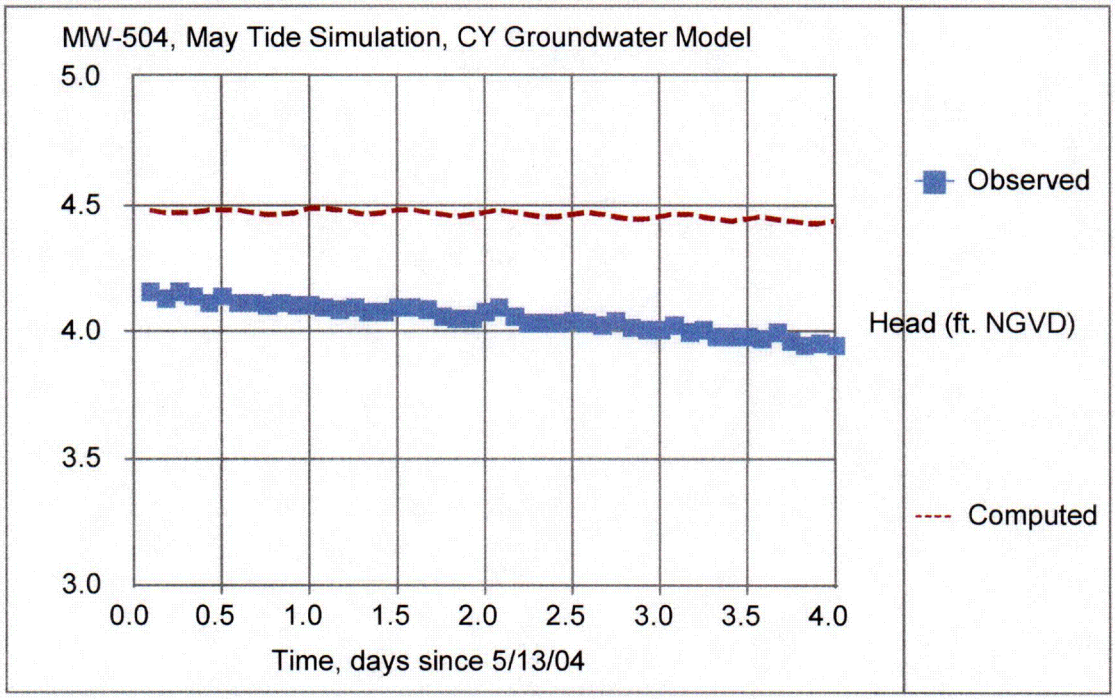
MW-504, May Tide Simulation, CY Groundwater Model
5.0
4.5
4.0
3.5
3.0
0.0
0.5
1.0
1.5
2.0
2.5
3.0
3.5
4.0
Time, days since 5/13/04
Observed
Computed
Head (ft. NGVD)

(o)

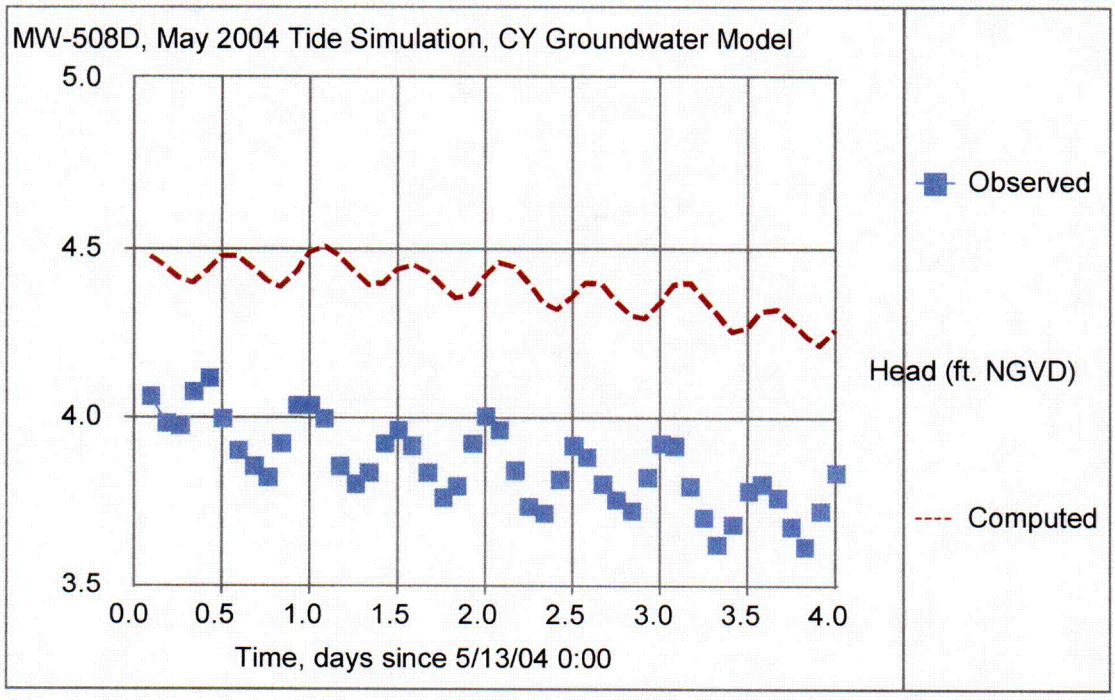
MW-508D, May 2004 Tide Simulation, CY Groundwater Model
5.0
4.5
4.0
3.5
0.0
0.5
1.0
1.5
2.0
2.5
3.0
3.5
4.0
Time, days since 5/13/04 0:00
Observed
Computed
Head (ft. NGVD)

(p)

Figure 22

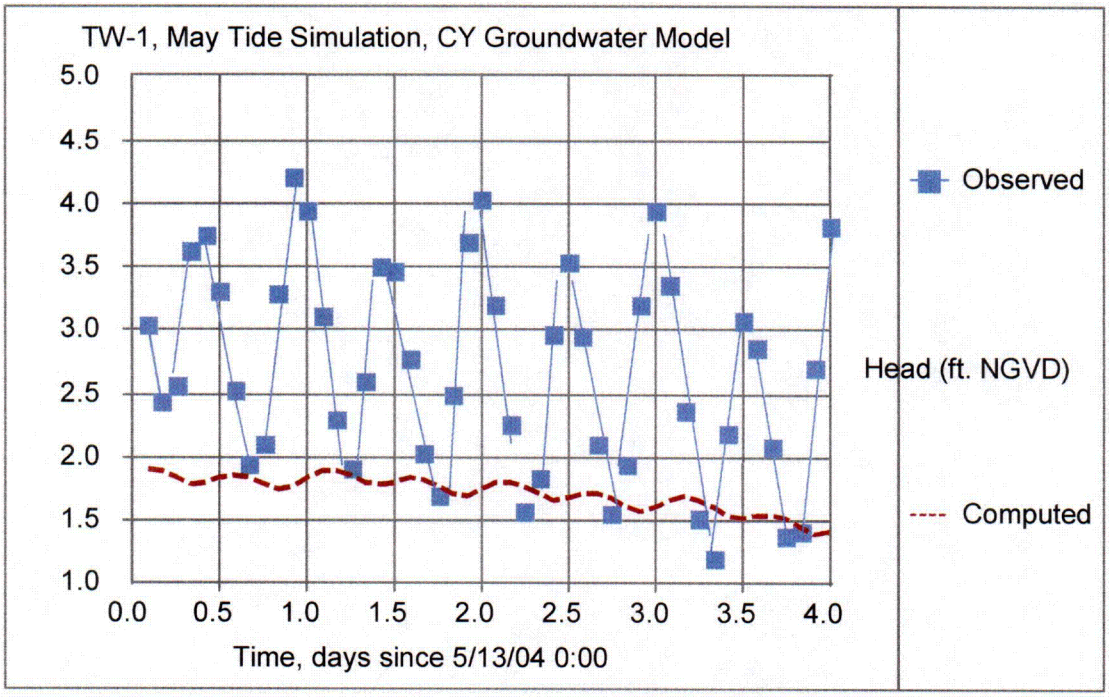
TW-1, May Tide Simulation, CY Groundwater Model
5.0
4.5
4.0
3.5
3.0
2.5
2.0
1.5
1.0
0.0
0.5
1.0
1.5
2.0
2.5
3.0
3.5
4.0
Time, days since 5/13/04 0:00
Observed
Head (ft. NGVD)
Computed

(q)